

RESEARCH ARTICLE

Daily energetic expenditure and energy consumption of short-finned pilot whales

William T. Gough^{1,*}, Brijonnay C. Madrigal^{1,2}, Augusta Hollers¹, Jens J. Currie^{1,3}, Robin W. Baird⁴, Kristi L. West⁵, Andreas Fahlman^{6,7,8}, Frank E. Fish⁹, Lewis Evans¹, Martin van Aswegen¹, Brian Stirling³, Aude Pacini¹, Grace L. Olson³, Stephanie H. Stack^{3,10}, Ashley M. Blawas¹¹, William A. Walker¹² and Lars Bejder^{1,13}

ABSTRACT

Diving is one of the most important behaviors undertaken by marine mammals. Pilot whales (Globicephala spp.) are oceanic dolphins that regularly forage at extreme depths (~600–1000 m) and maintain body sizes similar to beaked whales. They are also listed as data deficient, with little known about their population dynamics. To help fill this knowledge gap, we estimated their energetic demands through a combination of multiple data streams (e.g. unoccupied aerial systems photogrammetry, high-resolution accelerometry tag data, stomach content analysis and long-duration dive data from satellite tags) from short-finned pilot whales (Globicephala macrorhynchus) in Hawaiian waters. We estimated and compared pilot whale field metabolic rates from breathing frequency against a more granular cost of transport method developed from morphometrics and swimming kinematics, finding that these methods gave similar estimates of energetic expenditure during foraging dives. We then combined expenditure and intake estimates into an exploratory model of daily net energetic balance. Using an estimate of prey size derived from squid beaks collected from a stranded animal, we found that an average of 142±59.8 squid day⁻¹ (52,000±21,800 squid year⁻¹) is enough for an average adult short-finned pilot whale to reach a neutral net energetic balance. This species has an estimated population abundance of ~8000 individuals in Hawaiian waters, suggesting that the population as a whole would require 416±175 million squid (at an average of 559±126 kJ squid⁻¹) or approximately 88,000±37,000 tonnes of squid annually, assuming similar energetic requirements for each animal.

¹Marine Mammal Research Program, Hawai¹i Institute of Marine Biology, University of Hawai¹i, Mānoa, Kaneohe, HI 96744, USA. ²Scripps Institution of Oceanography, University of California San Diego, La Jolla, CA 92037, USA. ³Pacific Whale Foundation, Wailuku, Maui, HI 96793, USA. ⁴Cascadia Research Collective, Olympia, WA 98501, USA. ⁵Human Nutrition, Food and Animal Sciences, University of Hawai¹i, Honolulu, HI 96822, USA. ⁶Fundacion Oceanografic, Carrer d'Eduardo Primo Yúfera, 1B, 46013 Valencia, Spain. ⁵IFM, Linköping University, Olaus Magnus väg, 583 30 Linköping, Sweden. ⁶Global Diving Research SL, Valencia 46004, Spain. ⁶West Chester University, West Chester, PA 19383, USA. ¹ŌSouthern Ocean Persistent Organic Pollutants Program, School of Environment and Science, Griffith University, Nathan, QLD 4111, Australia. ¹¹Hopkins Marine Station, Stanford University, Pacific Grove, CA 93950, USA. ¹²Soophysiology, Department of Bioscience, Aarhus University, Aarhus 8000, Denmark.

*Author for correspondence (wgough@hawaii.edu)

D W.T.G., 0000-0003-2701-5299; B.C.M., 0000-0002-3592-8111; J.J.C., 0000-0001-6084-3091; R.W.B., 0000-0002-9419-6336; K.L.W., 0000-0003-3160-4598; A.F., 0000-0002-8675-6479; F.E.F., 0000-0001-5973-3282; L.E., 0009-0003-3744-7738; M.v.A., 0000-0001-6180-967X; B.S., 0000-0003-2938-8611; A.P., 0000-002-5691-8385; G.L.O., 0000-0002-7738-575X; S.H.S., 0000-0002-7199-8408; L.B., 0000-0001-8138-8606

Received 7 November 2024; Accepted 1 September 2025

ADDITIONAL LANGUAGE ABSTRACT

'O ka lu'u 'ana iho nō kekahi hana nui loa o nā mammal kai. 'O ka nai'a pailaka (Globicephala spp.) kekahi o nā nai'a e alualu pinepine ma ka hohonu nui (~600-1000 m), a nui nō ko lākou kino e like me ka nai'a nukunuku. Nele nō ho'i lākou i ka 'ike pili 'ole, a li'ili'i ka 'ike o ke 'ano o ko lākou lehulehu. I mea e ho'omāhuahua ai i ua 'ike nei, koho mākou i ko lākou pono mea 'ai ma o kekahi mau kumu 'ike (e la'a me, ka pa'i ki'i 'ana o ka helekopa uila li'i, ka mea pa'a 'ike ho'ohikiwawe, pio mea 'ai mai loko o ka 'ōpū, a me ka mea pa'a 'ike wā lō'ihi satellite) mai ka nai'a pailaka kualā pōkole (Globicephala macrorhynchus) ma nā kai Hawai'i. Ua koho a hoʻohālikelike mākou i ka nui o nā mea 'ai i hoʻolilo 'ia i ka ikaika e ka hanu mai ka nui o ka hanu 'ana me kekahi 'ano hana o ka ikaika e pono ai ka holo 'ana e ho'ohana ana i ke 'ano o ke kino a me ka holo 'ana. Like nā koho o ka nui o nā mea 'ai i ho'olilo 'ia i ka ikaika e ka hanu o kēia mau 'ano hana i nā lu'u alualu. A laila, ho'ohui mākou i nā koho o ka mea 'ai i ho'ohana 'ia a 'ai 'ia ma kekahi kumu o ka ho'okaulike mea 'ai no ka lā. Ua loa'a ke koho o ka nui o ka pio mea 'ai mai nā nuku mūhe'e i loa'a mai kekahi nai'a i ili, ua hō'ike mākou, lawa nō 142±59.8 mūhe'e lā ⁻¹ (52,000±21,800 mūhe'e makahiki⁻¹) no ka ho'okaulike mea 'ai o kekahi makua nai'a pailaka kualā pōkole. Ma kahi o 8000 paha ka nui lehulehu ma Hawai'i nei, e kuhikuhi ana, pono ka lehulehu holoʻokoʻa i 416±175 miliona mūheʻe (ma ka waena o 559±126 kJ mūhe'e⁻¹), a i 'ole 88,000±37,000 kona o ka mūhe'e i kēlā me kēja makahiki, me ka mana'o 'ja, like ka pono o ka mea 'aj no kēlā me kēia nai'a.

KEY WORDS: Energetics, Cetacean, Kinematics, Diving, Foraging

INTRODUCTION

Energy is the primary currency of life. The efficiency with which an individual acquires, converts and expends energy greatly influences its fitness (Boyd and Hoelzel, 2002; Chimienti et al., 2020; Crossin et al., 2014). Maintaining a positive balance of energetic intake to expenditure allows for the performance of basic physiological maintenance as well as complex, energy-intensive processes such as growth, reproduction and migration (Christiansen et al., 2018; Riekkola et al., 2020; Sebens, 1982; van Aswegen et al., 2025a,b). By contrast, a negative energetic balance results in adverse effects on the individual (e.g. decreased lipid stores, lowered immune function) or population (Demas and Nelson, 2012; Kebke et al., 2022; Martin et al., 2008; Svedäng and Wickström, 1997). Adaptations that increase the efficiency of energetic intake relative to costs can boost the capacity to perform essential functions, improve reproductive success and strengthen resilience to natural or human-induced disturbances (Goldbogen et al., 2019; Gough et al., 2022; Noren and Williams, 2000; van Aswegen et al., 2024; Videsen et al., 2023).

Deep-diving marine species such as sperm whales (Physeteroidea; Gray 1868), beaked whales (Ziphiidae; Gray 1850), and pilot

whales (*Globicephala*; Lesson 1828) may be living on an energetic 'knife-edge' (Goldbogen et al., 2019; Fahlman et al., 2025), foraging at extreme depths (1000–3000 m) (Aoki et al., 2017; Baird et al., 2003; Schorr et al., 2014) while needing to return to a 'central place' (i.e. the surface) to regain oxygen and offload CO₂ (Boyd, 1997). This life history strategy may make them especially vulnerable to disturbances (e.g. anthropogenic noise, climate change) that can disrupt foraging activities or increase energetic expenditure, leaving less margin for survival. Consequently, cost-saving measures and efficient foraging strategies become essential, allowing these species to minimize energetic expenditure while maximizing food intake and sustaining long dives (Czapanskiy et al., 2021; Goldbogen et al., 2019)

Among these species of deep-diving toothed whales (Odontoceti; Flower 1867), the sperm whale and beaked whales have attracted significant attention in recent years. This has resulted in studies of their dive behavior and physiology (Aoki et al., 2007; Hooker et al., 2009; Irvine et al., 2017; Martin López et al., 2015; Miller et al., 2004a; Pabst et al., 2016; Quick et al., 2020; Velten et al., 2013; Fahlman et al., 2025), foraging habits and diet (Aoki et al., 2012; Evans and Hindell, 2004a; Gaskin and Cawthorn, 1967; Gómez-Villota, 2007; Johnson et al., 2004; Santos et al., 2001; Southall et al., 2019; Watwood et al., 2006; West et al., 2017), growth and reproduction (Alves et al., 2023; Eguiguren et al., 2023; Evans and Hindell, 2004b; Feyrer et al., 2020; Kasuya, 1977, 1991; Miller et al., 2013; Nishiwaki et al., 1963; Ohsumi, 1965), response to disturbance (Czapanskiy et al., 2021; Farmer et al., 2018; Hin et al., 2023; Kvadsheim et al., 2012) and energetic balance (New et al., 2013; Silva et al., 2024).

In comparison to these extreme groups, pilot whales (short-finned, Globicephala macrorhynchus; long-finned, Globicephala melas) are data deficient across much of their range (Minton et al., 2018a,b). This is in spite of the fact that pilot whales have relatively large population sizes (Rogan et al., 2017; Wade and Gerrodette, 1993), are widely distributed in both deep slope and offshore waters (Cooke and Klinowska, 1991; Minton et al., 2018a,b) and maintain known foraging locations (Mahaffy et al., 2015; McComb-Turbitt et al., 2021; Meyer et al., 2024), making them more predictable to encounter than highly cryptic species such as beaked whales (MacLeod, 2018). Pilot whales are also unusual among oceanic dolphins (Delphinidae; Gray, 1821), foraging at up to ~1700 m on squid and fish (Aguilar Soto et al., 2008; Baird, 2016; Hernández-Garciá and Martín, 1994; Luna et al., 2024; Mintzer et al., 2008; Owen et al., 2019; Quick et al., 2017a; Ridgway, 1986; Schorr et al., 2022; Shearer et al., 2022) whereas other delphinid species typically forage closer to the surface (Arranz et al., 2019; Fahlman et al., 2023; West et al., 2018).

Both species of pilot whale are similarly sized to beaked whales [pilot whales: ~3–6 m; (Kasuya and Matsui, 1984); beaked whales: ~3–10 m; (MacLeod, 2005)], but show marked differences in physiological parameters (e.g. maximum dive depth, aerobic dive limit, muscle fiber structure) and behavior (e.g. repetition rate of foraging clicks) during foraging (Aguilar Soto et al., 2008; Johnson et al., 2005, 2006; Quick et al., 2017b; Shearer et al., 2022; Velten et al., 2013). These differences likely affect how pilot whales and beaked whales acquire and expend energy, underscoring the need for targeted research to better understand their energetic strategies.

Estimating energetic expenditure in cetaceans has a long history, dating back to Krogh's (1934) seminal work using breathing frequency as a proxy for oxygen consumption and energy use in blue whales. Since then, this method has evolved and been used to calculate 'field metabolic rates' (FMRs) at intermediate time-scales (i.e. hours to days) for a range of species (Christiansen et al., 2023; Lockyer, 1981; Rojano-Doñate et al., 2018; Sumich, 1983; Videsen et al., 2023).

Despite the broad use of this methodology, significant inter-breath variability exists in breathing parameters (e.g. breath duration, maximum nares area, O₂ uptake) in free-swimming animals (Nazario et al., 2022; Roos et al., 2016), suggesting that a simple count of breaths may not be enough to give an accurate determination of energetic expenditure. For animals housed under human care, this context has been provided through methods such as direct measurement of oxygen consumption (Allen et al., 2022; Williams and Noren, 2009), analysis of doubly labeled water (Rojano-Doñate et al., 2018) or the use of movement proxies such as overall dynamic body acceleration (ODBA) (Allen et al., 2022).

Swimming kinematics and relevant hydrodynamic metrics have also been quantified for animals housed under human care (Fish, 1998), allowing for crossover to wild populations through the measurement of mechanical thrust (Gough et al., 2021). These values of thrust can be converted into metabolic energetic expenditure during active swimming using simple assumed efficiency constants for propulsion (~90%; Gough et al., 2021) and metabolism (~25%; Massaad et al., 2007; Potvin et al., 2021; Gabaldon et al., 2022). Using fine-scale movement data from biologging tags with on-board inertial sensors (e.g. accelerometers, gyroscopes), it becomes possible to quantify active swimming kinematics as well as gliding periods of free-swimming animals (Gabaldon et al., 2022; Goldbogen et al., 2019; Gough et al., 2019, 2021; Martin López et al., 2015), allowing for differential calculation of energetic expenditure between uncontrolled movement states.

In addition to expenditure, energetic intake for echolocating whales can be determined through a combination of acoustic foraging signals ('buzzes') (Johnson et al., 2004; Watwood et al., 2006), and high-speed accelerometer signatures associated with prey capture attempts ('jerks') (Simon et al., 2012). The rate of foraging buzzes produced in a period of time has been used as a proxy for overall foraging attempts (Aguilar Soto et al., 2008; Miller et al., 2004b; Shearer et al., 2022; Wisniewska et al., 2016), with accelerometry being used as a method for isolating successful attempts from failures (Aguilar Soto et al., 2008; Shearer, 2022; Wright et al., 2021). Combining acoustic and kinematic data from biologging tags with data from stomach contents and measurements of prey calorific content allows for the estimation of energetic intake.

Previous research on the diving behavior of short-finned pilot whales has identified a distinct 'island-associated' pattern of foraging behavior, with fewer dives and fewer foraging attempts performed at higher speeds than other short-finned pilot whales foraging along continental slopes (e.g. Cape Hatteras; Alves et al., 2013; Aguilar Soto et al., 2008; Shearer et al., 2022). We hypothesized that the population of short-finned pilot whales in Hawai'i would forage in a similar manner, with cost-saving behaviors (i.e. descent gliding) making this high-risk, high-reward foraging strategy energetically viable (Aoki et al., 2017; Fahlman et al., 2023; Miller et al., 2004a; Narazaki et al., 2018; Visser et al., 2021). In this study, we use a combination of animal-attached tag (short- and long-term deployments) and UAS photogrammetry (unoccupied aerial systems, i.e. drones) data to quantify the diving behavior and estimate the energetic expenditure of short-finned pilot whales in Hawai'i. We then compare these values against a simplified estimate of FMR for each animal derived from breathing frequency, allowing us to outline the benefits and caveats of our expanded method. Finally, we combined our energetic expenditure estimates with information on prey species from a stranded animal, daily dive rates from satellite tag data and acoustic estimation of prey capture rates to generate a first-pass model that allows for individual and population-wide estimation of prey consumption and energy extraction from Hawaiian

waters. From this model, we found that an average of four squid per dive (142±59.8 squid day⁻¹; 52,000±21,800 squid year⁻¹) is enough for an average adult short-finned pilot whale to maintain a neutral net energetic balance. In order to assist future research, we have also outlined some of the primary caveats and sources of uncertainty in the model what could be enhanced with additional data.

MATERIALS AND METHODS

Data collection and processing

We deployed suction-cup attached multi-sensor CATS (customized animal tracking solutions) biologging tags on short-finned pilot whales (n=8) during daylight hours from a small boat (<30 m in length) using a 4-m-long carbon fiber pole following tagging procedures outlined by Friedlaender et al. (2009) and Wiley et al. (2011). Animals chosen for tagging were identified visually during dedicated surveys of a known deep-water region (~1000–1500 m) approximately 15 km southwest of the island of Lāna'i (Hawai'i, USA; Fig. S1). To minimize the influence of our research vessel, we quickly moved away from each tagged animal post-deployment and monitored their behavioral state from afar (>100 m with engines off) for 15–20 min. The deployments from 2023 and 2024 were set with 2-3 h galvanic timed releases to avoid tag loss. Each CATS tag included an inertial measurement unit (IMU) with a suite of sensors used to measure orientation (i.e. tri-axial accelerometer, tri-axial magnetometer, tri-axial gyroscope), pressure, light and temperature. These sensors are outlined by Cade et al. (2021). Sampling rates for the tri-axial accelerometers were set at 400 Hz to assist with measurement of forward swimming speed throughout the deployment following methods outlined by Cade et al. (2018). Sampling rates for the triaxial magnetometers and gyroscopes were set to 50 Hz. All other sensors were set to 10 Hz. Tags contained a single HTI-96-min hydrophone recording at a sampling rate of 96 kHz with hydrophonespecific sensitivity ranging from 169.4 to 170.2 re. 1 V µPa⁻¹. As part of the data processing procedure, sampling rates of all sensors (minus the acoustic recordings) were decimated down to 10 Hz (Cade et al., 2021). Tags also contained cameras set at 2K resolution, with LED headlights set to turn on at depth with a low-light trigger. For each tagged animal, we used a UAS flown at ~25 m altitude to record highresolution videos for the purpose of photogrammetry (Christiansen et al., 2016). Morphometrics were collected from these videos for each tagged animal using a DJI Inspire 2 quadcopter with either a Zenmuse X5s or X7 camera to record high-resolution video (3840×2160). A LightWare SF11/C laser altimeter was mounted on the UAS to simultaneously record altitude. Table 1 outlines general and morphometric information for each deployment.

For our energetic analyses, we incorporated daily dive rate data from 13 dart-attached depth-transmitting satellite tags (SPLASH10 and SPLASH10F, Wildlife Computers) deployed on short-finned pilot whales across the Hawaiian islands (Fig. S1; Table S1). We

also included prey size data obtained from stomach content analysis of a short-finned pilot whale that stranded in Hawai'i in 2014. All estimated numbers of squid consumption rely on this single sample, a notable caveat in our model.

All data were collected under appropriate NOAA NMFS/MMPA permits (no. 15330, 18786, 20605, 21321, 21476, 26596, and 27099) and university or Cascadia Research Collective IACUC protocols. UAS flights were operated by Part-107 authorized pilots in compliance with standards set by the Federal Aviation Administration.

CATS tag data

Kinematic and video analyses

From inspection of depth data, we identified 100 m as a cutoff that separated deep foraging dives (n=118) from shallow dives and surface behavior. This definition for deep dives has been previously used by Alves et al. (2013). Using processed sensor data from each animal, we counted the number of deep (>100 m) foraging dives using: (1) a depth of 2 m as a breakpoint between surface and diving and (2) a minimum dive duration of 3 min. For these foraging dives, we used the first and last negative-to-positive pitch changes occurring at >85% of the maximal dive depth to delineate the boundaries between the descent, bottom, and ascent phases. For each foraging dive, we measured the duration (s), maximal depth (m), mean and maximal swimming speed (m s⁻¹), and diel period of occurrence (day or night). We normalized each phase of the dive (descent, bottom, and ascent) to a 0–1 scale to account for differences in dive duration. In this scale, 0 represents the start of the phase (e.g. surface for descent, beginning of the bottom phase, and end of the bottom phase for ascent), while 1 represents the end of the phase (e.g. the beginning of the bottom phase for descent, end of the bottom phase, and surface for ascent). This allowed us to visually compare inter-dive kinematic trends, independent of dive duration.

Across each deployment, we defined active swimming and gliding periods and quantified a series of kinematic measurements for tailbeats using methods outlined by Gough et al. (2019, 2021). These included the duration (T_{beat} ; s) oscillatory frequency (f; Hz) and a series of swimming speed (m s⁻¹) measures for each tailbeat. These speed values included the starting speed (U_{s}), the final speed (U_{f}), the mean speed across the tailbeat (U_{avg}), and the change in speed between the start and end of the tailbeat (ΔU).

For a subset of dives, we used these tailbeats to manually identify the first and last transition points between active swimming and gliding during the descent and ascent phases, respectively. We also used custom MATLAB (R2022a; MathWorks, Natick, MA, USA) code from the Github repository 'respdetect' (Blawas, 2025) to detect breaths during surface periods and calculate an overall respiration rate ($R_{\rm resp}$; breaths min⁻¹) across each deployment (total respirations/total duration of deployment). For the single deployment in our dataset with >24 h of data (Gm221116-J2), we compared hourly dive rates between day and night hours as well as maximal foraging dive depths and

Table 1. Information on CATS tag deployments and related UAS-derived morphometrics for each tagged whale

ID	Deployment location	Deployment start–end (DD/MM/YYYY HH:MM) HST	Duration (h)	Age class	Total length (m)	Body mass (kg)	Chord length (m)	Fluke planar area (m²)	Surface area (m²)	Max. body diameter (m)	Fineness
Gm211005-86	20.7484N, 157.1074W	05/10/2021 09:10 h-05/10/2021 15:24 h	6.23	Adult	3.54	622.1	0.23	0.16	4.23	0.56	6.34
Gm211006-87	20.6945N, 157.0635W	06/10/2021 11:30 h-06/10/2021 11:55 h	0.42	Subadult	2.50	211.2	0.19	0.09	2.36	0.42	6.02
Gm221116-J2	20.7622N, 157.2222W	16/11/2022 13:10 h-18/11/2022 20:00 h	41.35	Adult	4.56	1186.5	0.31	0.28	6.07	0.66	6.93
Gm231109-J4	20.6944N, 157.0997W	09/11/2023 07:51 h-09/11/2023 10:32 h	2.68	Subadult	2.65	295.2	0.20	0.11	2.63	0.46	5.79
Gm231110-J6	20.6387N, 157.0710W	10/11/2023 07:28 h-10/11/2023 10:05 h	2.62	Adult	3.47	528.9	0.24	0.15	4.11	0.54	6.43
Gm231113-J5	20.7543N, 157.0878W	13/11/2023 10:15 h-13/11/2023 12:58 h	2.72	Adult	3.51	598.9	0.28	0.20	4.18	0.59	5.93
Gm240409-J3	20.6157N, 157.0617W	09/04/2024 09:18 h-09/04/2024 12:04 h	2.75	Adult	3.38	702.8	0.27	0.17	3.94	0.50	6.71
Gm240409-J4	20.6201N, 157.0650W	09/04/2024 09:09 h-09/04/2024 11:29 h	2.32	Adult	4.52	1183.9	0.35	0.28	6.00	0.78	6.34

Fineness=total length/maximum body diameter.

durations between dives occurring during the day and at night. In addition to kinematic parameters, CATS tag video was analyzed for instances of visible prey. Kinematic analyses were conducted using custom-written scripts in MATLAB (R2024a).

Acoustic analyses

Acoustic data from six deployments were excluded from our acoustic analyses owing to low signal quality, high noise levels and variable tag specific hydrophone sensitivity, which limited identification of signals produced by the focal animal. For the other two deployments (Gm231109-J4, Gm231113-J5), we identified presumed foraging attempts as the end positions of acoustic 'terminal buzz' signatures. To find these signatures, we segmented the large acoustic file (.wav) for each deployment into 1 h files in Adobe Audition 2022 [1024 fast Fourier transform (FFT), Hann 50% overlap] to improve processing time and accessibility. Next, an experienced analyst visually and aurally scanned spectrograms of successive 1 h files for each deployment in Raven Pro 1.6 to detect the presence of terminal buzzes [clicks with an inter-click interval (ICI) of <0.02 s] following a series of regular clicks (ICI >0.1 s) (Pedersen et al., 2021). Analyses were conducted using custom-written scripts in MATLAB (R2021a). For buzz detection, the start and end times of buzzes were manually selected from spectrograms (512 FFT, Hann 50% overlap). Nonbuzz clicks were detected using an energy detector to detect clicks produced by the focal animal (threshold=23.5 dB). The detector parameters were selected based on a subset of clicks to confirm optimal classification rate. Click parameters calculated included ICI (ms) and timing relative to kinematic data. Clicks produced by the focal animal (tagged individual) were distinguished from non-focal animals based on higher amplitude click energy in the low frequencies (15 kHz) (Arranz et al., 2016; Johnson et al., 2006). Therefore, a band-pass filter was applied to the detector to eliminate low frequency noise and non-focal animal click energy in the higher frequencies to improve detector performance. To check for high-speed foraging sprints, we determined the maximal speed within a five second window (±2.5 s) of the end of each buzz. A sprint was defined as a spike to >3 m s⁻¹ (Aguilar Soto et al., 2008). To differentiate sprints from high-acceleration spikes unrelated to forward movement, we overlaid our swimming speed from tag 'jiggle' with jerk and, for periods where the animal was pitched >20 deg, the swimming speed derived from orientation-corrected depth rate (OCDR; Miller et al., 2004a; Fig. S2). True sprints would show spikes or elevated portions in all three metrics.

UAS morphometric analyses

For each CATS-tagged animal, we selected nadir images from UASderived videos where the full body (i.e. head, dorsum, tail flukes) was visible at or very near the water's surface. Subsequent morphometric analyses were performed using MorphoMetriX V2 (Torres and Bierlich, 2020) and Whalength (Dawson et al., 2017). For each animal, we measured the total body length (L_{total} ; m), the body width at the widest point $(W_{\text{max}}; m)$, the chord length of the tail from fluke insertion to notch ($L_{\rm chord}$; m) and the planar fluke area ($A_{\rm fluke}$; m²) using methods outlined by Gough et al. (2021). We then calculated body volume using methods outlined by Arranz et al. (2022). To estimate body mass (M_b, kg) , we multiplied body volume by the mean body density (1038.8 kg m⁻³) reported for long-finned pilot whales using hydrodynamic gliding models (see Aoki et al., 2017, for methods). To account for the contribution of gas components, we applied a body density correction factor following the approach of Glarou et al. (2023) using a mean air volume estimate of 34.6 ml kg⁻¹ from Aoki et al. (2017).

Satellite tag data - dive rate analyses

The depth-transmitting satellite tags provide summary information on durations of dives and 'surface' periods, and maximum depths for all dives exceeding a user-defined depth threshold. Blocks of time spent above this threshold (50 m) are categorized as surface periods. For each dive and surface period, the tags transmit two duration values (in seconds), which typically vary by just a couple of seconds; we used the mean of the two duration values to determine the combined amount of surface and dive data for rate calculations. Similarly, for the maximum depth of each dive, two values are sent, a minimum and maximum, and we used the mean of these two values to determine the number of dives that exceeded 99.5 m (i.e. ≥100 m). The daily dive rate for each individual was calculated as the number of dives ≥100 m per day of combined dive and surface data.

Stomach content data - prey size analyses

On 6 July, 2014, a stranded short-finned pilot whale in advanced decomposition was reported dead at Kualoa, Oʻahu. The carcass was recovered and necropsied on 7 July, 2014. The total body length was 513 cm and confirmed as adult male based on size of the testes. Cause of death was not determined at necropsy and diagnostics were limited by the state of decomposition. Stomach contents were collected and frozen. Significant marine debris that included fishing gear was noted among the food items in the stomach but gastric obstruction was not observed.

Prey remains were later thawed and rinsed through a progression of sieves with decreasing mesh sizes of 1.4 mm, 0.94 mm and 0.50 mm. After sorting, squid beaks were preserved in 70% ethanol. Squid beaks were identified to the lowest possible taxon using the private reference collection of W.A. Walker and the squid beak reference collection housed at the National Marine Mammal Laboratory, Seattle, WA, USA. The total number of each species of squid was estimated as the number of lower beaks present. Prey item condition allowing, lower beak rostral lengths of squid were measured to the nearest 0.1 mm using an optical micrometer or vernier calipers. Where possible, prey size was estimated by applying appropriate regressions to these measurements in order to determine individual prey mass (Clarke et al., 1985; Wolff, 1982). In cases where length/mass regression equations for a particular prey species were unavailable, individual mass was estimated through comparison with appropriately sized museum specimens or by comparison with other closely related species of similar size.

Energetic expenditure

We estimated energetic expenditure ($E_{\rm expend}$; J) for each CATS-tagged animal by combining morphometrics with fine-scale swimming kinematics (averaged over each individual tailbeat cycle). To start, we calculated the reduced frequency (σ) using the equation:

$$\sigma = \frac{\omega L_{\text{chord}}}{U_{\text{avg}}},\tag{1}$$

where ω is the angular frequency of fluking (ω =2 πf). Next, we calculated the feathering parameter (θ) using the equation:

$$\theta = \frac{\alpha U_{\text{avg}}}{\omega h},\tag{2}$$

which constitutes the ratio between the maximum angle between the chordwise plane of the flukes (i.e. leading to trailing edge) and the direction of motion [α ; set at 30 deg as outlined by Fish (1998) and Gough et al. (2021)] and the maximum angle ($\omega h/U_{\rm avg}$) achieved by

the trajectory of the pitching axis of the flukes (Chopra and Kambe, 1977) when reaching the amplitude of heave (h; m). Peak-to-peak amplitude has been measured as one-fifth of body length for a range of oscillatory swimmers (e.g. fish, cetaceans) and has been found to be unchanging across a range of swimming speeds (Bainbridge, 1958; Fish, 1998; Gough et al., 2019). The heave amplitude (h) was defined as the midline-to-peak displacement, equivalent to half the peak-to-peak amplitude, and set as one-tenth of body length. We used cubic interpolation [via SciPy's 'griddata' package (Virtanen et al., 2020)] to generate a set of surface plots from lunate-tail propulsion data (Chopra and Kambe, 1977). With these plots, we were able to estimate the coefficient of thrust (C_t) and propulsive efficiency (μ_{prop}) for a given combination of ω and θ values. For each tailbeat period, we calculated mean thrust power output (P_T ; J s⁻¹) using the equation:

$$P_{\rm T} = 0.5 \rho C_{\rm T} U_{\rm avg}^3 A_{\rm fluke} \left(\frac{h}{L_{\rm chord}}\right)^2, \tag{3}$$

where ρ is the density of seawater (set to 1025 kg m³ at 25°C). To convert $P_{\rm T}$ into mean metabolic power ($P_{\rm met}$; J s⁻¹), we used the equation:

$$P_{\text{met}} = \frac{P_{\text{T}}}{\mu_{\text{met}}\mu_{\text{prop}}},\tag{4}$$

where the aerobic efficiency (μ_{met}) ranged from 0.1 to 0.4 to capture plausible variation in the conversion of muscle chemical energy to mechanical work (Fish, 1996; Potvin et al., 2021). To confirm the accuracy of our hydrodynamic modeling, we used our estimates of $C_{\rm T}$ and $P_{\rm T}$ to calculate corresponding drag coefficients and drag forces and compare these 'active' measurements against 'passive' drag measurements for a body of a given shape moving through the water (see Supplementary Materials and Methods).

To determine the overall energetic expenditure of a given time period (Eexpend; J), we conducted a Monte Carlo simulation with 1000 iterations. Within each iteration, we perturbed α and our calculated h for each tailbeat period (within a $\pm 10\%$ range) to account for uncertainty in the kinematics of the tail, then we propagated those values through our hydrodynamic modeling to allow for realistic variability in our estimation of $P_{\rm T}$. From there, we randomly selected values for μ_{met} , basal metabolic rate (BMR; J s⁻¹), and the heat increment of feeding (HIF; J s⁻¹). The range for BMR was set using the Kleiber (1975) relationship ($70 \times M_{\rm b}^{0.75}$; kcal day $^{-1}$), converted to J s $^{-1}$ via 1 kcal day $^{-1}$ =0.04843 J s $^{-1}$. The HIF was centered at 15% of BMR (Rechsteiner et al., 2013). Given our limited knowledge of the uncertainty surrounding these variables, we allowed both to vary $\pm 10\%$ from their respective baseline values. For the period of interest, we summed P_{met} across all seconds of active swimming, then added BMR and HIF for the entire period (during active swimming and passive gliding) to account for maintenance and digestive costs. We refer to these methods as the 'thrust' method and we include a selection of modelrelevant parameter values for each deployment in Table 1.

For each Monte Carlo iteration, we generated a full time-series (0.1 s resolution) of $E_{\rm expend}$ using the thrust method. Across all iterations, we calculated a median expenditure time-series with 5th–95th percentile bounds. We also calculated per-second $E_{\rm expend}$ values for each foraging dive ('diving') as well as an overall persecond cost for diving, for the time spent outside deep foraging dives (i.e. surface and shallow diving; 'non-diving'), and for the entire deployment (referred to as 'deployment'). In order to do this, we summed the cost for seconds spent in the particular dive or behavioral state (e.g. diving, non-diving, deployment) and divided

them by the duration of that particular dive or behavioral state. We then averaged the per-second costs for each dive and for each behavioral state across all Monte Carlo iterations for each deployment to generate means (\pm s.d.) and confidence intervals (5% and 95%) for use in subsequent analyses. To account for variability due to body size, we also report mass-specific values of $E_{\rm expend}$ (J s⁻¹ kg⁻¹).

Ås a comparison to the thrust method, we estimated per-second deployment-level FMR values on both an absolute (kJ s $^{-1}$) and mass-specific (kJ s $^{-1}$ kg $^{-1}$) basis using a combination of measured respiratory rates ($R_{\rm resp}$) and physiological values obtained from previous modeling efforts on larger (Videsen et al., 2023) and smaller (Fahlman et al., 2016; Isojunno et al., 2018) cetaceans (see Supplementary Materials and Methods). We refer to this simplified secondary method as the 'breathing frequency' method. Similarly to the thrust method, we accounted for uncertainty in parameter estimates by implementing a Monte Carlo simulation (100 iterations) and sampling from defined ranges. Final estimates of $E_{\rm expend}$ represent the mean (\pm s.d.) and confidence intervals (5% and 95%) across these iterations.

It should be highlighted that the breathing frequency method is: (1) partly based on parameters from baleen whales and other small cetaceans, and (2) assumes values for model variables that do not vary with behavioral state or level of exertion. This has been a criticism of the method and suggests that it is only useful for long-term estimation of metabolic rates (Fahlman et al., 2016). Despite these limitations, the breathing frequency method provides us with a way to compare $E_{\rm expend}$ at the deployment-level between two vastly different methodological approaches.

To assess the sensitivity of each model to its input parameters, we generated data-frames that included all available combinations of input variables. From these, we plotted the effects of varying each parameter on deployment-level $E_{\rm expend}$ with all other parameters held constant (Fig. S3).

Energetic intake and daily net energetic balance

Details of our data-streams and energetic modeling are presented schematically in Fig. 1. To estimate daily net energetic balance $(E_{\text{net}}; \text{kJ})$, we began by modeling daily energetic intake $(E_{\text{intake}}; \text{J})$ as a function of prey size $(M_{\text{prey}}; \text{g} \text{ wet-weight})$, calorific content $(\text{Cal}_{\text{prey}}; \text{kJ g}^{-1})$, assimilation efficiency $[\mu_{\text{assim}}; \text{set at } 90\% \text{ (Lockyer, } 1993)]$, deep foraging dives performed per day $(N_{\text{dives}}; \text{dives day}^{-1})$ and presumed prey capture events per dive $(N_{\text{prey}}; \text{captures dive}^{-1})$:

$$E_{\text{intake}} = M_{\text{prey}} \text{Cal}_{\text{prey}} \mu_{\text{assim}} N_{\text{dives}} N_{\text{prey}}. \tag{5}$$

To account for potential variation in diving behavior and prey capture success, we generated anchored ranges for our variables ($\pm 25\%$), then conducted a Monte Carlo simulation by drawing 10,000 random combinations of input values to produce a distribution of $E_{\rm intake}$ estimates. We anchored $M_{\rm prey}$ at 211.9 g, using the median size of prey items found in the stomach of a freshly stranded Hawaiian short-finned pilot whale (n=341 squid beaks from 27 species; K.L.W., unpublished data). We anchored Cal_{prey} at 2.925 kJ g⁻¹ using an average of wet weight calorific content values from eight species of squid (Clarke et al., 1985). We anchored $N_{\rm dives}$ at 38.5 dives day⁻¹ using the mean of the individual daily dive rates from our satellite tag deployments (Table S1). We attempted to use our acoustic data to generate an anchor for $N_{\rm prey}$, but the number of deep foraging dives with terminal buzzes in our dataset (n=5 from two tagged individuals) was limited and each dive took place during

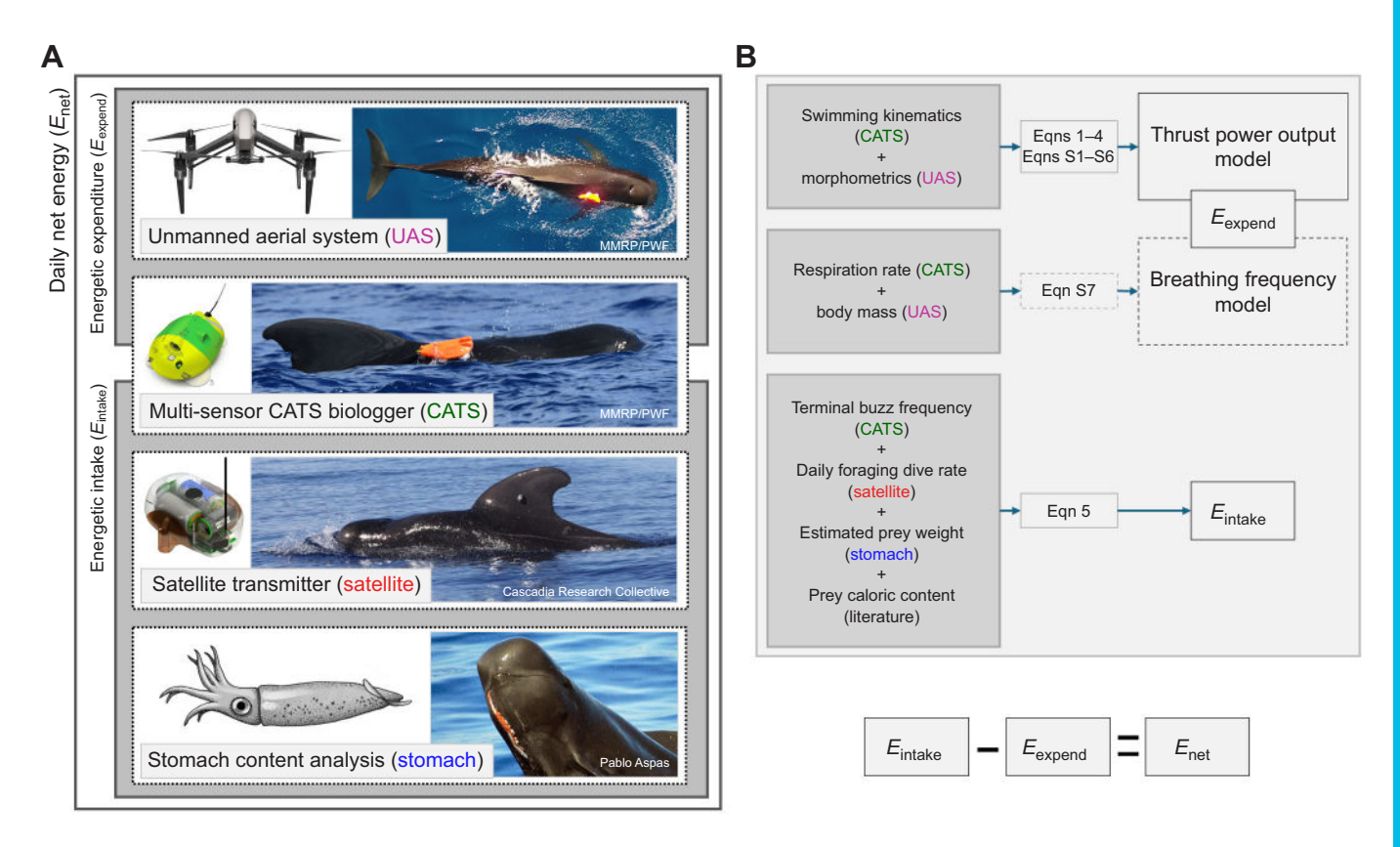


Fig. 1. Methodological schematic for data types and energetic modeling in the short-finned pilot whale. (A) The four primary data types in our analyses: UAS-photogrammetry, CATS tag deployments, stomach content analysis and satellite tag deployments. (B) Schematic synthesis showing how our data are used in the various equations to generate estimates of E_{expend} and E_{intake} .

the same period in the late morning. Instead, we incorporated per-dive buzz rate estimates from the literature (Aguilar Soto et al., 2008; Shearer et al., 2022) to create a potential range (1–15) of per-dive prey capture events. To determine the impact of these prey capture rates on overall energy intake, we ran additional Monte Carlo simulations (10,000 iterations) for each level of $N_{\rm prey}$, generating a distribution of possible $E_{\rm intake}$ values for each prey capture scenario.

For each simulated $E_{\rm intake}$ value, we generated a corresponding value of daily $E_{\rm expend}$ using our thrust method by combining persecond cost estimates for diving and non-diving behavioral states with the percentage of the day spent in each behavioral state. To do this, we started by randomly sampling average per-second cost estimates and average dive duration estimates from normal distributions parameterized by the mean and standard deviation of deployment-level means from the eight tagged individuals in our dataset. Daily $E_{\rm expend}$ was the sum of: (1) the cost of diving, calculated as $N_{\rm dives}$ multiplied by mean dive duration and per-second diving cost, and (2) the cost of non-diving time, calculated as the remaining seconds in a 24 h period multiplied by the per-second non-diving cost. Subtracting each $E_{\rm expend}$ value from its corresponding $E_{\rm intake}$ (Eqn 6) resulted in an overall distribution of $E_{\rm net}$ as well as one for each capture rate scenario (1–15 prey captures dive⁻¹).

$$E_{\text{net}} = E_{\text{intake}} - E_{\text{expend}} \tag{6}$$

Statistical analyses

All statistical analyses were performed in R (version 4.0.5; r-project. org) using the *stats* and *lme4* (https://CRAN.R-project.org/package=lme4) packages. Linear relationships were coded as 'ordinary-least-squares' regressions. Two-tailed *t*-tests were used to

compare day and night hours for hourly diving rates, maximal foraging dive depths, and foraging dive durations (in min) in the single deployment (Gm221116-J2) that lasted for >24 h. Prior to conducting t-tests, we assessed normality using the Shapiro-Wilk test and homogeneity of variances with Levene's test. Normality was confirmed for maximal dive depths and dive durations during both the day and night as well as the dive rate during the day, but the dive rate at night deviated slightly from normality. Levene's test showed homogeneity of variances for all three metrics during the day and night, so we proceeded with Welch's two-tailed t-tests. Significance levels were set to 0.05 throughout our analyses. Average values are reported as means±s.d., unless otherwise stated. To account for high variability between deployments (e.g. duration, dive count, etc.), we calculated mean values for kinematic and energetic parameters for each individual, then reported the mean of those individual means where appropriate.

RESULTS

Diving behavior

Monitoring of tagged animals after deployment suggested that they all returned to their pre-tagging behavioral state within 5–10 min, giving us confidence that our presence and the process of tagging had not affected their behavior. The majority of our deployments were short (≤ 3 h), with one deployment (Gm211005-86) lasting ~ 6 h and the longest deployment (Gm221116-J2) lasting ~ 41 h before the tag stopped recording data (the tag stayed attached for another ~ 10 h). The deepest (864 m) and longest duration (18.9 min) foraging dives were achieved by Gm221116-J2 (Table 2). In this deployment, we found variation in the frequency of foraging dives between daytime (n=25; 1.47 ± 1.28 dives h⁻¹) and night-time (n=67;

Table 2. Metrics related to deep foraging dives (>100m) performed by each CATS tagged whale

	Foraging			Buzz dives	Dep	Respiration rate			
ID	dives (>100 m)	Max. depth (mean±s.d.) (m)	Max. duration (mean±s.d.)(min)	(no. of buzzes)	No. dives with gliding	Descent (m)	Ascent (m)	Difference (m)	(breaths min ⁻¹)
Gm211005-86	7	838 (724±71)	14.28 (13.77±0.63)	0	7	49.56±9.00	27.87±2.24	21.69±9.87	1.99
Gm211006-87	1	185 `	6.13	0	1	35.54	17.05	18.49	2.05
Gm221116-J2	92	864 (465±194)	18.87 (12.60±3.12)	0	42	62.17±18.50	59.40±8.71	12.97±14.31	1.66
Gm231109-J4	2	624 (592±46)	10.02 (9.65±0.53)	2 (7)	2	43.84±15.73	30.16±6.06	13.68±9.67	1.89
Gm231110-J6	6	502 (337±124)	7.12 (5.20±1.35)	0 `	2	24.74±7.35	34.39±4.12	9.65±11.48	2.22
Gm231113-J5	5	814 (711±66)	16.15 (15.52±0.65)	3 (10)	5	44.30±9.83	37.65±1.58	7.70±7.65	2.08
Gm240409-J3	4	619 (329±204)	11.55 (9.58±1.53)	0 `	4	78.83±35.77	29.90±8.43	48.93±33.60	1.54
Gm240409-J4	1	525	14.02	0	0	_	_	_	1.80
Total	118	621.38±225.79 (483.50±191.93)	12.27±4.40 (10.81±3.79)	5 (17)	63	48.43±17.70	33.77±13.00	19.02±14.04	1.90±0.23

Buzz dives, number of dives with hydrophone buzzes. Where appropriate, total values are either shown as sums or means±s.d.

2.58 \pm 1.70 dives h⁻¹) hours (t=-2.427; d.f.= \pm 40.1; P=0.02). We also found a difference in the maximal depths of foraging dives occurring during the day (\pm 602.6 \pm 170.2 m) and at night (\pm 13.8 \pm 177.6 m) (\pm 4.677; d.f.= \pm 44.8; Φ <0.001) as well as a difference in the duration of foraging dives occurring during the day (\pm 1.85 \pm 2.68 mins) (\pm 3.614; d.f.= \pm 35.8; Φ <0.001). Across all individuals, we found an average maximal foraging dive depth of \pm 484 \pm 192 m and an average foraging dive duration of \pm 4.8 min. In addition to our CATS tag data, we calculated a daily dive rate of \pm 48.9 dives day⁻¹ from our satellite tag dataset (\pm 13 deployments; Table S1). Fig. 2 shows the relationship between maximal dive depth and dive duration, as well as the difference

between dives occurring during the day and at night. We found a positive linear relationship between duration and maximum depth of a foraging dive (y=-116.5+48.84x, $R^2=0.69$).

We found a distinct pattern of active stroking and gliding during the descent and ascent phases (Figs 3 and 4A–C). On the descent, individuals would actively beat their tail for the first $\sim 10\%$ of the descent, at which point they would cease stroking and glide until they reached the end of the phase at depth. This transition occurred at an average depth of 48.4 ± 17.7 m. On the ascent, this pattern would reverse, with individuals actively stroking for the majority of the phase and transitioning to a glide at an average depth of 33.8 ± 13.0 m. We found an average difference of 19.0 ± 14 m between these transition

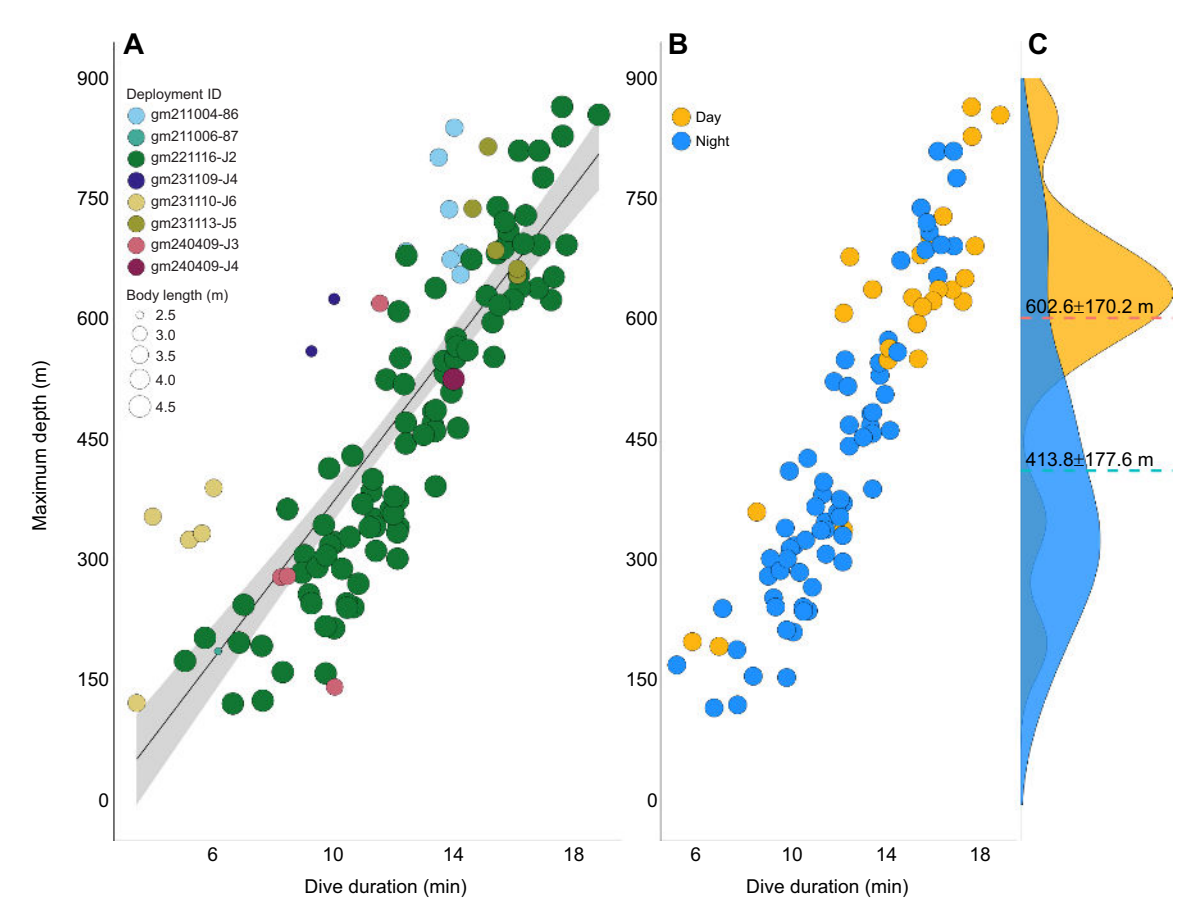


Fig. 2. Relationship between dive duration (min) and the maximal dive depth (m). (A) Full dataset of foraging dives (n=118), with size denoting the total body length of each animal. (B) Foraging dives (n=92) from our single long deployment (Gm221116-J4), split between day and night. The plot along the right-hand side shows the density of dive depths during the day and at night, with horizontal dotted lines denoting mean maximal dive depths.

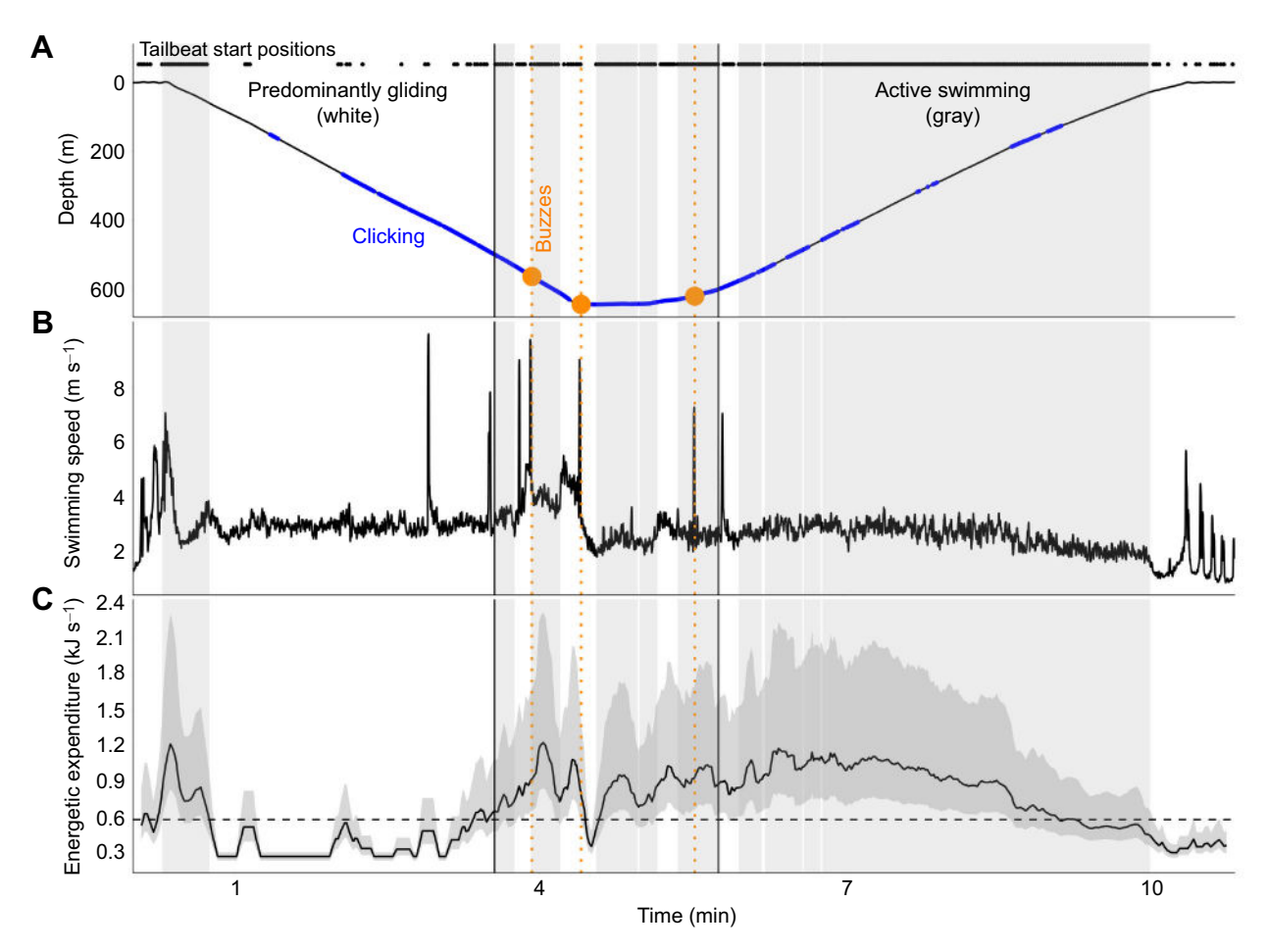


Fig. 3. Overview of a single foraging dive performed by short-finned pilot whale Gm231109-J4. Subplots show the depth (A), jiggle-derived swimming speed (B) and instantaneous energetic expenditure estimates (C) for the full period of the dive. Blue segments along the depth trace represent acoustic click production, while orange circles and dotted lines denote the timing of foraging buzzes derived from acoustic data. Gray segments correspond with periods (>10 s) of active swimming; white corresponds with unpowered gliding. Black circles along the top denote the start times of individual tailbeats. For the fine-scale energetic expenditure estimates from our thrust method, the solid line denotes the median of bootstrapped samples and the dark gray bounds denote the 5% to 95% confidence interval. The dotted line corresponds to the mean deployment-scale energetic expenditure estimate from our breathing frequency method.

points during the descent and ascent phases. This beat-and-glide pattern corresponded with higher swimming speeds (Fig. 4D–F) and subsequently higher energetic expenditure during the active swimming portions of the dive (Fig. 4G–I).

We found six instances of suspected prey presence on the video. These constituted: (1) an object moving toward the head of the animal or (2) a brightly-illuminated object moving past the camera that was presumed to be a cloud of squid ink (Fig. 5E). Two of our suspected prey instances aligned in time with acoustic terminal buzzes (Buzz 1 and Buzz 2 in Fig. 5).

Acoustic foraging buzz and clicking behavior

We searched for acoustic signatures ('buzzes') from a total of seven foraging dives (two from Gm231109-J4 and five from Gm231113-J5) in a combined 5.4 h of on-animal data. We found that 71% of those dives (n=5) had at least one terminal buzz in the acoustic record, with an average of 2.43 ± 1.72 buzzes dive⁻¹ across all seven dives and a total of 17 buzzes across all dives. The buzzes produced by Gm231109-J4 (n=7; 41% of total) were associated with moments of high swimming speed (up to 7.9 ± 1.9 m s⁻¹). All of these buzzes displayed spikes in the jiggle-derived swimming speed and jerk, but not in the OCDR-derived swimming speed (Fig. S2), suggesting a short-duration, high-acceleration movement such as a prey capture

instead of a movement-associated sprint (i.e. a pre-capture prey chase). The buzzes produced by Gm231113-J5 (n=10) did not display highspeed moments (mean maximal speed=1.86±0.28 m s⁻¹). Buzzes were produced at an average dive depth of 615±89 m. Signals produced by Gm231109-J4 were high enough quality for further click analysis. The onset of non-buzz clicks produced by the animal began at 300-400 m with maximal clicking in the 400-600 m depth range during the ascent and descent phases. A total of 2593 clicks were detected during the descent, bottom, and ascent phases of both foraging (≥100 m) and non-foraging (<100 m) dives [excluding surface time (<2 m depth) owing to high false positive rate caused by interaction with the water surface]. Most clicks were produced in the descent and ascent, with the lowest number of clicks produced during the bottom phase of non-foraging dives. Median ICI during the descent and ascent phases were 0.25±0.14 s and 0.20±0.23 s, respectively. Table S2 includes a sample of literature sources that include relevant acoustic metrics (i.e. diving buzz rates, non-buzzing ICIs).

Energetic expenditure

As a validation of our thrust method, we found deployment-level active-to-passive drag ratios ranging from 2.73 to 10.6, with an average of 5.88 ± 3.2 (see Table S3). For our calculation of energetic expenditure on a per-second basis (thrust method; $E_{\rm expend}$), we

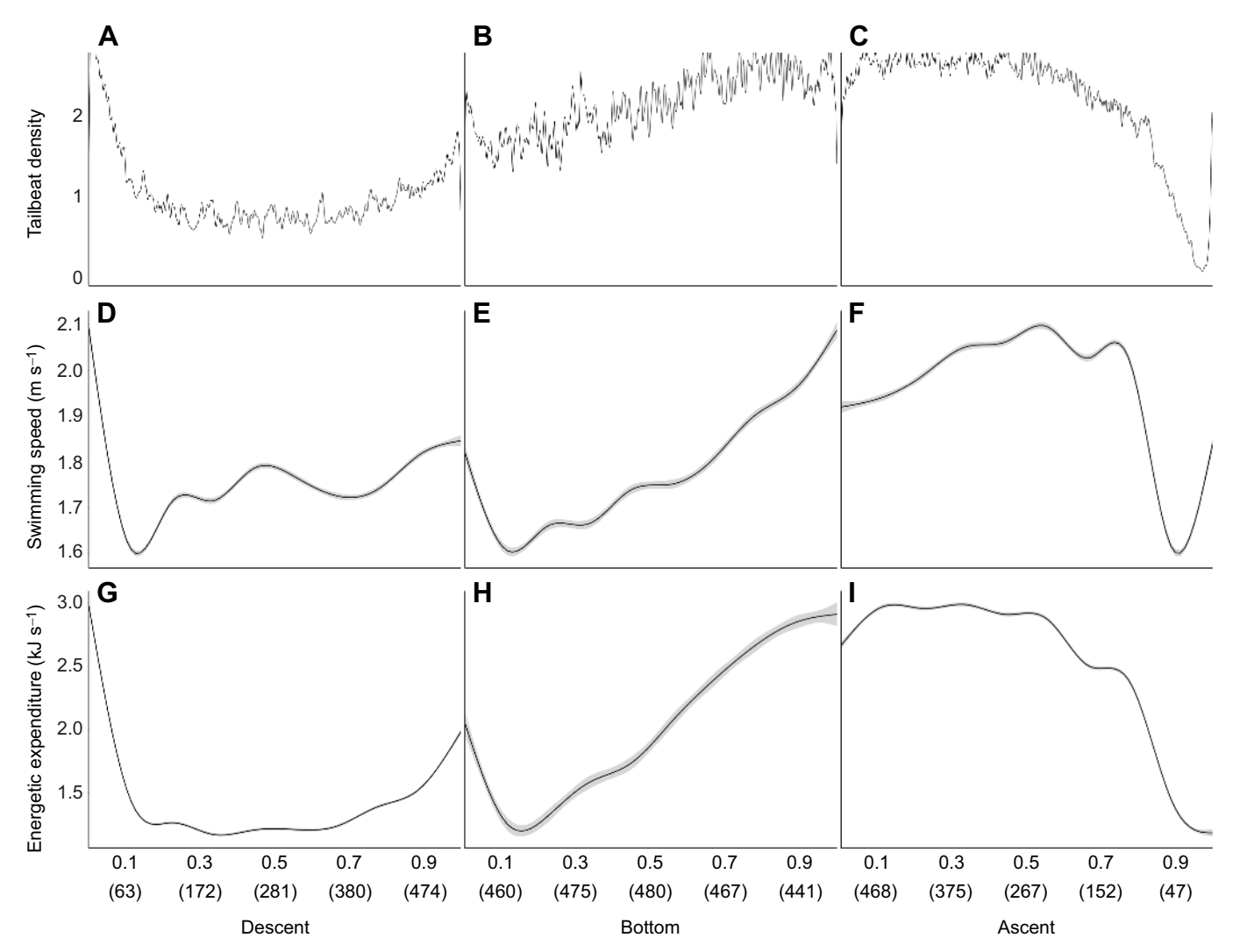


Fig. 4. Normalized descent, bottom and ascent phases of a dive. Density plots of tailbeat start positions (A–C), swimming speed (D–F), and energetic expenditure from the thrust method (G–I) for all dives across all individuals in our dataset. Numbers in parentheses along the bottom correspond with the mean binned depth throughout each of the labeled 10% segments in the normalized dataset.

found a higher average value of $1.23\pm0.53~kJ~s^{-1}$ during foraging dives $(1.95\pm0.44~J~s^{-1}~kg^{-1})$, with a lower average value of $0.74\pm0.34~kJ~s^{-1}$ during non-diving periods $(1.16\pm0.16~J~s^{-1}~kg^{-1})$. At the deployment level, we found an intermediate average value of $0.90\pm0.42~kJ~s^{-1}~(1.41\pm0.21~J~s^{-1}~kg^{-1})$. In comparison, we found an average expenditure value of $1.23\pm0.55~kJ~s^{-1}~(1.94\pm0.29~J~s^{-1}~kg^{-1})$ using the breathing frequency method. This resulted in a median difference ($\pm s.d.$) between the two methods of $6.7\pm11\%$ during foraging dives, $41\pm5.5\%$ during non-diving periods and $29\pm5.6\%$ at the deployment level. Values for these energetic calculations are given in Table 3 and shown in Fig. 6.

We found positive linear relationships between body mass and average per-second energetic expenditure using both methods (thrust–diving: y=0.3205+0.001365x, R^2 =0.876; thrust–non-diving: y=0.139+0.000908x, R^2 =0.906; breathing frequency: y=0.2402+0.001485x, R^2 =0.942; Fig. 6A). On a mass-specific basis, we found slightly negative linear relationships between body mass and average per-second, per-kilogram energetic expenditure (thrust–diving: y=0.002372–6.288 $e^{-07}x$, R^2 =0.266; thrust–non-diving: y=0.001327–2.512 $e^{-07}x$, R^2 =0.307; breathing frequency: y=0.002332–5.823 $e^{-07}x$, R^2 =0.542; Fig. 6B).

Multi-scale energetic budgets

Cephalopods (n=27 species) accounted for >99% of the identifiable prey items (by mass) in the stomach of the stranded short-finned pilot whale included in our analyses. The median estimated mass (\pm s.d.) of these squid was 212 \pm 532 g wet weight, while the largest squid was estimated to be 7391 g. Combining this number with a calorific content of 2.92 kJ g⁻¹ and an assimilation factor of 90% resulted in an average of 559 \pm 126 kJ squid⁻¹ (134 \pm 30.1 kcal squid⁻¹).

From our prey capture rate-dependent distributions, we found that capture rates of four squid per dive resulted in approximately 50% of simulations achieving a positive energetic balance (Fig. 7A,C). To achieve this positive energetic balance, pilot whales in Hawai'i would need to consume 75.6±25.9 MJ day $^{-1}$ (5th–95th CI: 33–118) to match daily energetic costs ($E_{\rm expend}$) – equivalent to 142±59.8 squid day $^{-1}$ (CI: 56-251). The average $E_{\rm net}$ value from our overall Monte Carlo simulation was slightly higher (83.6±102 MJ day $^{-1}$ [CI: –59–269]) (Fig. 7B). This was likely due to our model including per-dive prey capture rates up to 15.

On an annual basis, these estimates would result in an extraction of 52,000±21,800 squid whale⁻¹ year⁻¹ (CI: 20,000–91,600) to

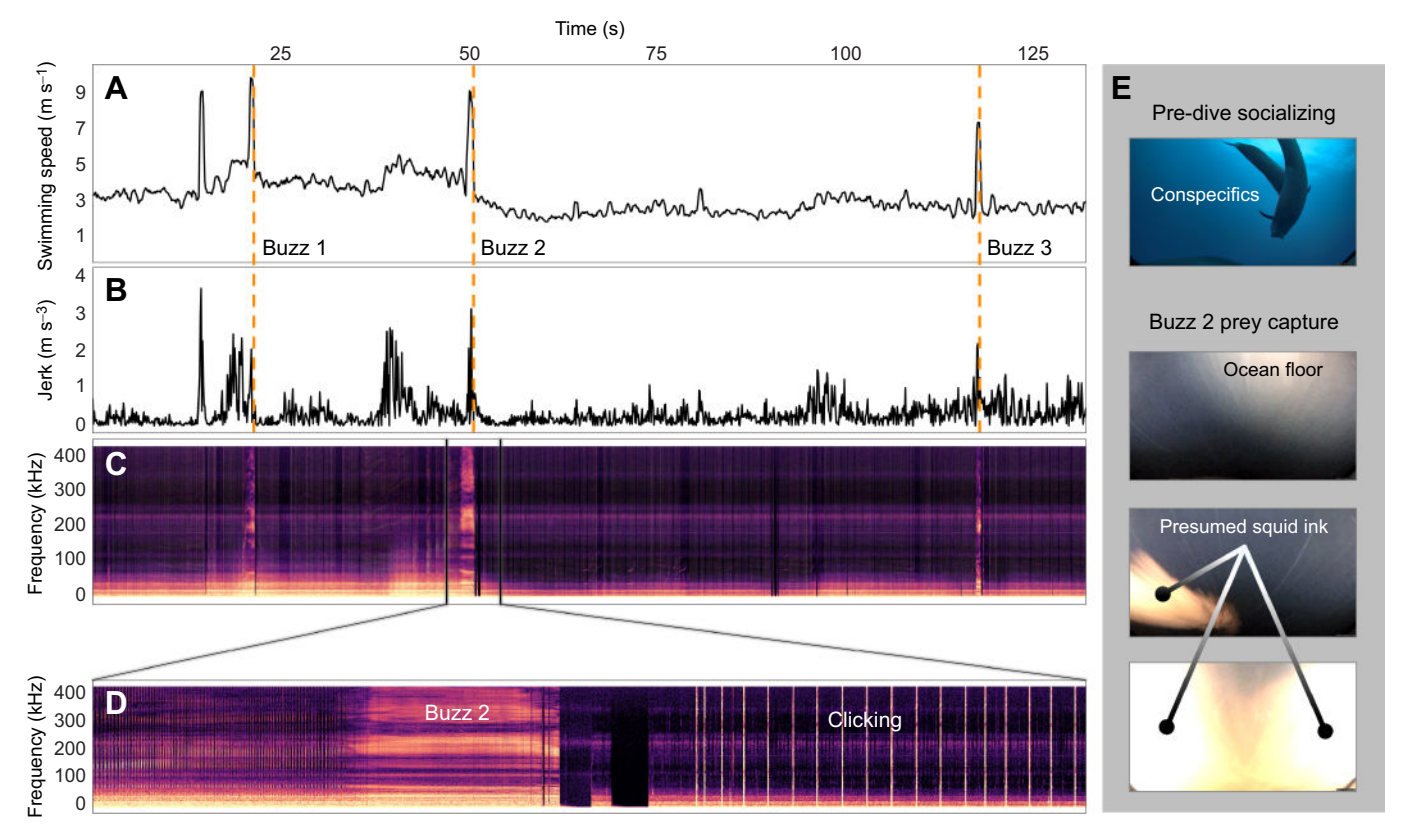


Fig. 5. Zoom segment of data around three foraging buzzes derived from acoustic data. Subplots show the jiggle-derived swimming speed (A), jerk (B) and spectrogram (C), as well as a further zoom period of the spectrogram (D) around one of the foraging buzzes (Buzz 2). Orange dotted lines denote the end positions of each buzz. (E) Images taken from the CATS video record and show conspecifics near the surface as well as the ocean floor and what appears to be a squid ink cloud appearing <2 s from the end time of Buzz 2.

cover $E_{\rm expend}$. A population size of 8000 individuals (Bradford et al., 2021) would result in a population-wide extraction of 416 \pm 175 million squid year⁻¹ (5th–95th CI: 160-733 million), or 88,000 \pm 37,000 tonnes of squid year⁻¹. At the lowest and highest ends of the estimated range of pilot whale abundance (~2700–23,300) given by Bradford et al. (2021), our model would result in population-wide extractions of 140 \pm 58.9 million squid year⁻¹ (5th–95th CI: 55–247 million) and 1.21 billion \pm 509 million squid year⁻¹ (5th–95th CI: 480 million–2.13 billion), respectively. These equate to 29,700 \pm 12,500 and 256,000 \pm 108,000 tonnes of squid year⁻¹, respectively.

DISCUSSION

The diving behavior of short-finned pilot whales has been described in a number of geographic regions (e.g. Cape Hatteras, Tenerife, Madeira, Hawai'i), but information on their energetic budget has remained scarce (Aguilar Soto et al., 2008; Alves et al., 2013; Baird, 2016; Shearer et al., 2022). This species is an important behavioral and physiological out-group for deep-diving species such as sperm whales and beaked whales, as well as being susceptible to disturbance and stranding at levels above those seen in other species (Hamilton, 2019; Parsons, 2017). For these reasons, understanding the cost of life and subsequent intake requirements of this species are of value to management and conservation efforts (Carretta et al., 2023). Previous estimates for this species have relied on comparisons with the closely related long-finned pilot whale (Hin et al., 2019; Isojunno et al., 2018; Lockyer, 1993). Our study is the first to combine high-resolution kinematic data with morphometrics and geographically linked information on daily

dive habits and prey intake to develop an approximation of daily prey requirements and overall energetic budgets.

Island-associated foraging in short-finned pilot whales

Our results on the average depth (~400–800 m) and duration (~8–16 min) of foraging dives broadly confirm similar trends for short-finned pilot whales shown in various geographic regions (e.g. Hawai'i, Cape Hatteras, Tenerife, Madeira) (Abecassis et al., 2015; Aguilar Soto et al., 2008; Alves et al., 2013; Baird et al., 2003; Owen et al., 2019; Shearer et al., 2022). The majority of these studies found diel diving patterns, with fewer dives to greater depths and more surface resting behavior observed during daylight hours, consistent with animals tracking the diel vertical migration of cephalopod prey (Watanabe et al., 2006; Young, 1978). Only one animal in our highresolution tag dataset had >24 h of data, but displayed a similar trend (Fig. 2B,C). Shearer et al. (2022) found the opposite relationship, with more foraging effort occurring during the day. This could be related to the Cape Hatteras population foraging on the continental slope, as opposed to the island-associated foraging on the mesopelagic boundary community that is seen in other studies (Mintzer et al., 2008).

This island-associated foraging strategy has been described by Aguilar Soto et al. (2008) as 'high risk, high reward' because of the presence of extremely high speed (9 m s⁻¹) sprints associated with the capture of large, mobile prey items. Shearer et al. (2022) also found sprints, but they occurred at slightly slower speeds (~7 m s⁻¹). Though our acoustic dataset was limited, we found elevated swimming speeds (~4 m s⁻¹) culminating in a jerk spike prior to the majority of acoustic buzzes from one individual (Gm231109-J4), but not the other (Gm231113-J5) (Fig. S2). The

Table 3. Energetic expenditure metrics for each CATS tagged whale using the thrust and breathing frequency methods

			Thrust [CI] (kJ s ⁻¹) (J s ⁻¹ kg ⁻¹) [CI]			Breathing frequency	Ratio (thrust/breathing frequency)				
ID	BMR (kJ s ⁻¹)	HIF (kJ s ⁻¹)	Foraging dives	Non-diving	Full deployment	[CI] (kJ s ⁻¹) (J s ⁻¹ kg ⁻¹) [CI]	Foraging dives	Non-diving	Full deployment		
gm211004-86	0.42±0.02	0.06±0.02	1.23±0.30	0.69±0.09	0.83±0.15	1.25±0.32	0.98	0.56	0.67		
			[0.89-1.86]	[0.58-0.89]	[0.66-1.15]	[0.78-1.82]					
			(1.97±0.49)	(1.12±0.15)	(1.34±0.23)	(2.00±0.51)					
			[1.43-2.99]	[0.93-1.43]	[1.06-1.84]	[1.25–2.92]					
gm211006-87	0.19±0.01	0.03±0.01	0.35±0.06	0.25±0.03	0.32±0.05	0.48±0.12	0.73	0.53	0.68		
_			[0.28-0.47]	[0.21-0.33]	[0.27-0.42]	[0.30-0.68]					
			(1.65±0.27)	(1.20±0.17)	(1.53±0.22)	(2.25±0.56)					
			[1.33–2.22]	[0.99–1.54]	[1.26–1.99]	[1.41–3.22]					
gm221116-J2	0.69±0.04	0.10±0.04	1.91±0.46	1.06±0.14	1.48±0.29	1.91±0.48	1	0.56	0.77		
			[1.39-2.86]	[0.89-1.34]	[1.14-2.08]	[1.23-2.79]					
			(1.61±0.39)	(0.90±0.11)	(1.24±0.24)	(1.61±0.40)					
			[1.18–2.41]	[0.75–1.13]	[0.96–1.76]	[1.04–2.35]					
gm231109-J4	0.24±0.01	0.04±0.01	0.76±0.20	0.34±0.04	0.42±0.06	0.60±0.15	1.27	0.57	0.69		
			[0.54-1.17]	[0.29-0.42]	[0.34-0.54]	[0.39-0.86]					
			(2.57±0.67)	(1.15±0.13)	(1.41±0.20)	(2.03±0.50)					
			[1.84–3.97]	[0.97–1.42]	[1.16–1.84]	[1.31–2.92]					
gm231110-J6	0.38±0.02	0.06±0.02	1.40±0.40	0.73±0.13	0.87±0.18	1.20±0.30	1.17	0.6	0.72		
-			[0.97-2.25]	[0.57-1.00]	[0.66-1.26]	[0.75–1.75]					
			(2.65±0.75)	(1.37±0.24)	(1.65±0.35)	(2.27±0.57)					
			[1.83-4.26]	[1.09–1.89]	[1.25–2.38]	[1.43–3.31]					
gm231113-J5	0.41±0.02	0.06±0.02	1.20±0.30	0.83±0.17	1.05±0.24	1.27±0.32	0.95	0.66	0.83		
			[0.87-1.83]	[0.64-1.19]	[0.78-1.55]	[0.79-1.86]					
			(2.01±0.50)	(1.39±0.28)	(1.75±0.40)	(2.12±0.54)					
			[1.45–3.06)	[1.07–1.98]	[1.30–2.58]	[1.33–3.11]					
gm240409-J3	0.46±0.03	0.07±0.03	1.10±0.24	0.74±0.10	0.83±0.13	1.08±0.27	1.02	0.69	0.77		
			[0.83-1.60]	[0.62-0.95]	[0.68-1.10]	[0.68-1.57]					
			(1.57±0.34)	(1.06±0.14)	(1.18±0.18)	(1.54±0.38)					
			[1.19–2.28]	[0.88–1.35]	[0.96–1.56]	[0.97–2.23]					
gm240409-J4	0.69±0.04	0.10±0.04	1.89±0.45	1.30±0.23	1.43±0.27	2.06±0.52	0.92	0.63	0.69		
-			[1.38-2.84]	[1.02-1.80]	[1.11–1.99]	[1.31–3.01]					
			(1.59±0.38)	(1.10±0.20)	(1.20±0.23)	(1.74±0.44)					
			[1.17–2.40]	[0.86–1.52]	[0.94–1.68]	[1.11–2.54]					
Mean±s.d.	0.44±0.18	0.06±0.03	1.23±0.53	0.74±0.34	0.90±0.42	1.23±0.55	6.70±11.03%	41.50±5.50%	29.04±5.569		

Bold values at the bottom represent the means±s.d. across individuals (median±s.d. for method ratios).

duration of these higher-speed segments was relatively short (\sim 5 s), suggesting that the animals were engaged in rapid prey capture events, as opposed to sustained 'sprinting' chases.

In conjunction with sprint speeds, the lower buzz rates seen in Tenerife (0.6–1.5 buzzes dive⁻¹; Aguilar Soto et al., 2008) in comparison to Cape Hatteras (11.7–14.7 buzzes dive⁻¹; Shearer et al., 2022) suggest that those animals may be relying on fewer, larger prey items to cover expenditure. Our acoustic dataset wholly consisted of daytime foraging dives, so we were unable to quantify diel changes in buzz rate for our Hawaiian population, but our mean daytime buzz rate (2.4±1.7 buzzes dive⁻¹) aligned more closely with the daytime buzz rates for Tenerife than with those from Cape Hatteras. Although we were unable to confirm the presence of high-speed foraging sprints, our results for buzz rates support the hypothesis that short-finned pilot whales in island environments display a distinct island-associated foraging strategy that is similar between geographic regions.

Central to this island-associated foraging strategy are squid, known for their highly migratory lifestyle from the deep ocean during the day up into shallower waters at night (Watanabe et al., 2006; Young, 1978). Stomach content analyses on pilot whales are sparse, but squid appear to be the dominant prey resource for short-and long-finned pilot whales around the world (Beasley et al., 2019; Hohn et al., 2006; Luna et al., 2024; Mercer, 1975; Mintzer et al., 2008; Overholtz and Gordon, 1991; Sinclair, 2006). In many of

these studies, squid were >90% of the prey found in the stomachs of stranded animals. Only Mintzer et al. (2008) found a more diverse set of small fish and squid (<20 g) from stranded animals in Cape Hatteras, a result that aligns with the higher buzz rates shown by Shearer et al. (2022) in that region. In contrast, Luna et al. (2024) found only squid in the stomachs of animals stranded in Tenerife, with a median estimated size of \sim 85 g. Data from long-finned pilot whales in Tasmania suggests even larger median prey sizes (\sim 130 g) (Beasley et al., 2019). Given this context, the median size of prey obtained from our Hawaiian animal (\sim 200 g) appears to be toward the larger end, with the largest squid found to be in excess of 7000 g.

Short-finned pilot whales versus other cetaceans

The diel diving patterns seen in island-associated short-finned pilot whale populations is not unique to this species, with sperm whales off the Ogasawara Islands displaying shallower, more frequent dives at night (Aoki et al., 2007). This species, as well as beaked whales, have a similar affinity for squid (Clarke et al., 1997; West et al., 2017), but they do not perform the same high-speed sprints as pilot whales, suggesting that their chosen prey species may be smaller or less mobile. West et al. (2017) found a median prey size of ~150 g for goose-beaked whales (*Ziphius cavirostris*), slightly smaller than our pilot whale estimate. Clarke et al. (1997) found an average sperm whale prey size of 923 g, but also a wide size

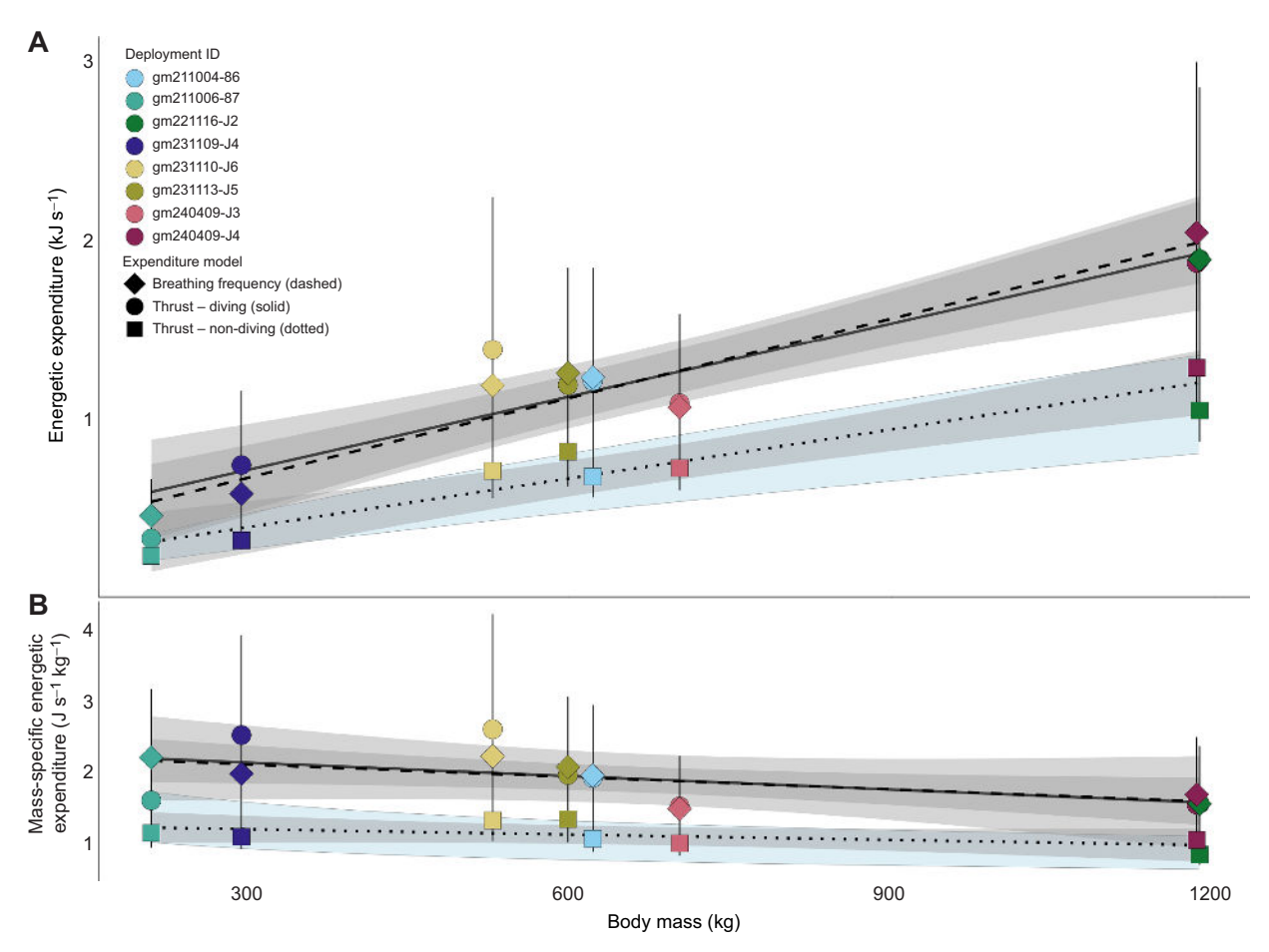


Fig. 6. Relationship between body mass and per-second energetic expenditure. (A) Absolute and (B) mass-specific energy expenditure. Both foraging dives (diving; filled circles, solid line) and non-diving periods (non-diving; filled squares, dotted line) were included for the thrust method, whereas the breathing frequency method did not differentiate between behavioral states (filled diamonds; dashed line). The blue shaded regions correspond with estimates of energetic expenditure taken from Lockyer (1993) for long-finned pilot whales (1.2–2.0 times Kleiber).

range from 100 to 100,000 g. Sperm whales are also significantly larger than either pilot whales or beaked whales (11–16 m; Whitehead, 2018), with different prey sizes being targeted by different sex and size classes. Our CATS tag dataset did not include enough variability to comment on those factors, although they are likely to play a role in pilot whale diving behavior and energetics.

Given a large potential range of prey sizes, odontocetes have been shown to preferentially forage on larger prey items, if available (MacLeod et al., 2006). Goldbogen et al. (2019) suggested that larger body sizes impart advantages (i.e. lower mass-specific metabolic rate and cost of transport), but that availability of prey at the upper end of that size range is ultimately a major factor limiting body size and energetic efficiency in deep-diving odontocetes. Czapanskiy et al. (2021), in studying the effects of short-term disturbance on a variety of cetacean species, similarly found that intermediate-sized animals such as pilot whales should be the least likely to suffer adverse effects due to loss of foraging opportunity. In contrast, the small harbor porpoise (Phocoena phocoena) must continuously feed (up to ~550 prey captures per hour) on smaller fish species to overcome their high metabolic demands (Rojano-Doñate et al., 2018, 2024; Wisniewska et al., 2016). By maintaining their intermediate size and foraging in known prey hotspots (Abecassis et al., 2015), pilot whales likely maximize their energetic efficiency and chance of encountering prey on a given dive.

This inference is supported by the strong relationship between dive depth and duration found in our current study (Fig. 2) and by Alves et al. (2013) in Madeira, with animals appearing to spend minimal time searching for prey at depth. This suggests that they are acoustically active and searching for prey during the descent phase, a behavior that has been shown for other cetaceans (Miller et al., 2004b). Our analysis of non-buzz clicking from Gm231109-J4 found that clicking started around 300–400 m on the descent, supporting this conclusion and aligning with previous work (Aguilar Soto et al., 2008). Clicking behavior is an echolocation strategy used by many species to perceptually filter out echoes from multiple targets and maintain long range detection during the descent (Madsen et al., 2005). Sperm whales and beaked whales start clicking at 100–200 m and 200–500 m, respectively (Johnson et al., 2005; Watwood et al., 2006).

Comparing energetic expenditure between thrust and breathing frequency methods

The active-to-passive drag ratio – comparing the drag generated by an actively swimming body to the parasitic drag on that same body during passive gliding – is a hydrodynamic variable that has been quantified for a wide range of aquatic species and swimming styles (Lighthill, 1971; Webb, 1975), generating a broad base of knowledge that we can use to validate that the thrust power estimates from our current analyses are realistic. Studies have found values as high as 16 for a Pacific white-sided dolphin (*Lagenorhynchus obliquidens*) (Webb, 1975) down to less than 1 for a fish-like robot (Barrett et al., 1999). Values at the lower end of this range have sparked debate, with proponents arguing that cetacean species

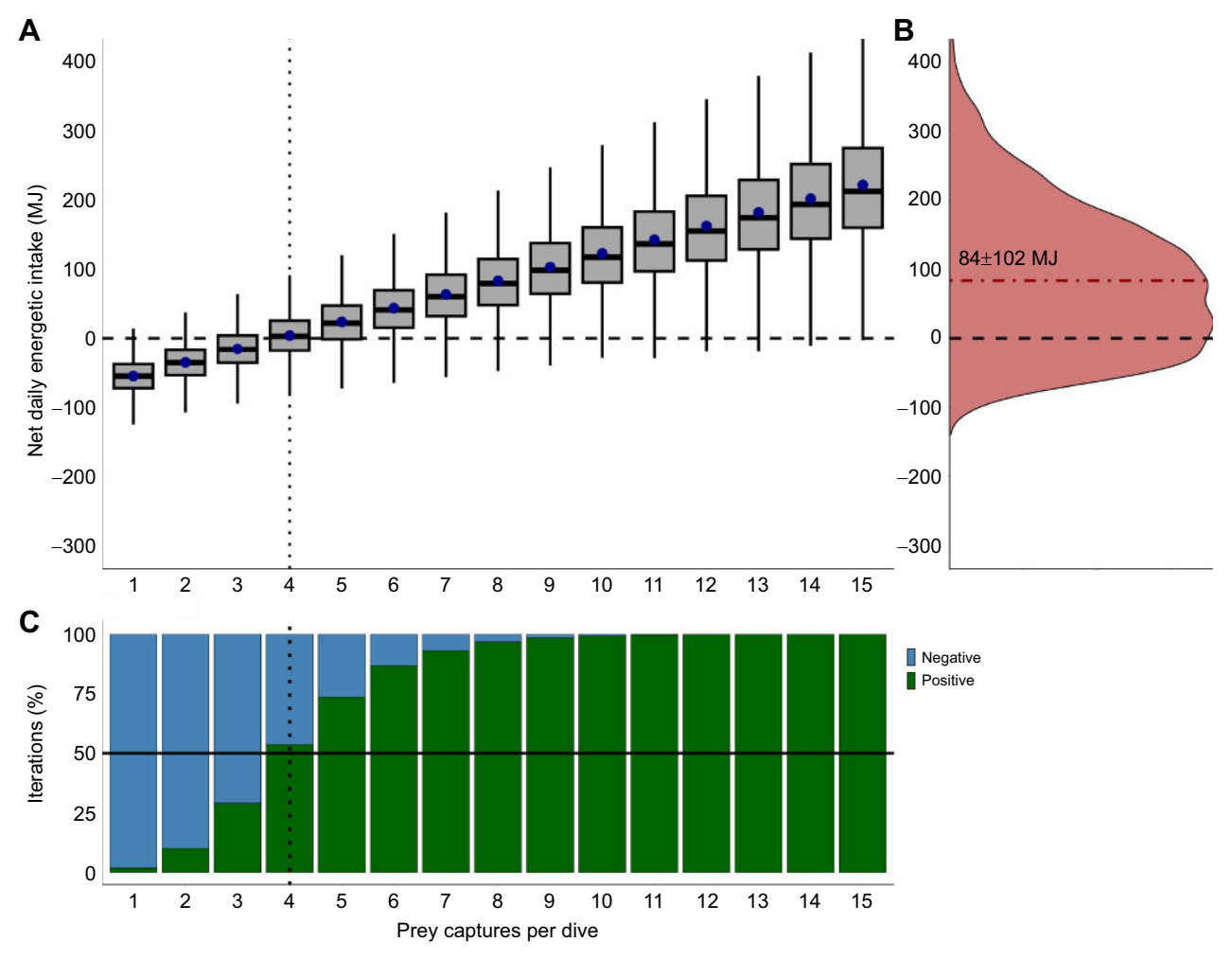


Fig. 7. Monte Carlo simulations showing net energetic intake. Simulations across a range of per-dive capture rates (A) and overall (B). The black horizontal dashed lines denote the zero-point where intake exactly balances expenditure. The red horizontal dot-dash line denotes the mean of our overall Monte Carlo simulation (annotated as mean±s.d.). Box and whisker plots show the median (middle line), quartiles (1st and 3rd), and ranges between the minimum and maximum values. Mean values for each distribution are over-plotted as blue circles. (C) Number of Monte Carlo simulation iterations (out of 10,000) that result in either a negative (blue) or neutral/positive (green) net energetic intake. The vertical dotted line denotes the lowest per-dive prey capture value (4) in which at least 50% of iterations resulted in a neutral/positive net energetic intake.

do not have the muscle mass required to overcome estimated drag, and instead possess unique drag reduction mechanisms (e.g. laminarization of the boundary layer) that allow for exceptionally low drag during active swimming (Barrett et al., 1999; Davis et al., 2024; Kramer, 1961, 1962; Parry, 1949). Opponents of this socalled 'Gray's Paradox' cite methodological flaws in James Gray's (1936) original study, instead suggesting that the active-passive drag ratio for cetaceans should follow established hydrodynamic principles and fall in line with other swimming animals (Fish, 2006; Fish et al., 2014; Webb, 1975). The measured values for our short-finned pilot whales (ranging from 2.73 to 10.6, with an average of 5.88±3.2) align more closely with the latter assertion, and fall within a similar range to the values found by Webb (1975) for the long-beaked common dolphin (Delphinus bairdii) (6.3) and Dall's porpoise (*Phocoenoides dalli*) (9.4), as well as the value found by Fish (1993) for the bottlenose dolphin (Tursiops truncatus) (3.2) and the assertion by Lighthill (1971) that active swimming should increase drag by 3–5 times over passive gliding. Given these findings, we suggest that the energetic values from our thrust method are a useful comparison against the breathing frequency method.

One of the primary goals of our study was to estimate the daily energetic budget of short-finned pilot whales, but we also hoped to use our integrative dataset to: (1) determine periods of high- and low-expenditure at a more granular scale using the thrust method and (2) estimate field metabolic rate from the breathing frequency method in a way that would be directly comparable to the body of literature that exists for other species. These two estimates aligned well, especially during foraging dives (6.7±11% different). As a comparison, Lockyer (1993) estimated the daily energetic expenditure of a 1000 kg long-finned pilot whale (Globicephala melas) to be $61,686-102,672 \text{ kJ day}^{-1} (0.71-1.19 \text{ kJ s}^{-1}), 1.2-2.0$ times the Kleiber (1975) estimate of basal metabolic rate for that species. Isojunno et al. (2018) found a similar daily estimate of 86,608 kJ day⁻¹ (1.00 kJ s⁻¹). These values are similar, but below the estimates from both of our methods (Fig. 6A), suggesting that our models have: (1) overestimated daily energetic expenditure, or (2) more accurately captured higher-exertion periods (e.g. dive ascents). Further investigation would be helpful to determine how behavioral factors are affecting these energetic estimates on a longer time scale. In addition to our absolute values, we found that massspecific energetic expenditure did not change greatly with body size (Fig. 6B), suggesting that future modeling efforts could extrapolate these per-kilogram values to individuals for whom there are body size estimates, but not enough additional data to perform the full thrust method.

In addition to our daily energetic expenditure values, the thrust method allowed us to determine which behaviors result in higher or lower energetic expenditure on a fine scale. The majority of studies on cetacean diving energetics rely on averaged field metabolic rate estimates over broader time scales and cannot parse high- and low-expenditure segments within a dive (Christiansen et al., 2023; Sumich, 1983; Videsen et al., 2023; Villegas-Amtmann et al., 2017), although some have used stroking rate or movement proxies such as the overall dynamic body acceleration (ODBA) to generate more accurate metabolic estimates for high- and low-exertion behaviors (Fahlman et al., 2023; Williams, 1999; Williams and Davis, 2024; Fahlman et al., 2025).

Short-finned pilot whales, like many other diving cetaceans (Fahlman et al., 2023; Miller et al., 2004a; Narazaki et al., 2018; Visser et al., 2021) as well as non-cetacean species such as white sharks (Watanabe et al., 2019) and pinnipeds (northern elephant seals; Aoki et al., 2011; California sea lions; Cole et al., 2023; Weddell seals; Williams et al., 2000), display a pattern of stroking and gliding to take advantage of negative buoyancy on the descent (Aoki et al., 2017). This strategy is often described as a costreducing measure, but that assertion has only recently been tested for bottlenose dolphins (Tursiops truncatus), finding greater amounts of acceleration (ODBA) and energy expenditure on the ascent versus the descent phase of the dive (Fahlman et al., 2023; Miller et al., 2012; Sato et al., 2013). We found similar differences in our thrust method estimate of expenditure, confirming that gliding does indeed reduce expenditure on the descent, but that the rapid stroking required to counteract negative buoyancy on the ascent overtakes those cost savings, resulting in a high net expenditure for deep foraging dives relative to time spent at or near the surface. Miller et al. (2012) predicted a similar pattern of diving energy use for animals that deviated sharply from neutral buoyancy. Interestingly, we found that the change from stroking to gliding occurred at a deeper depth during the descent as compared to the ascent. This suggests that pulmonary gas volumes may result in neutral buoyancy at similar depths on both the descent and ascent, with stroking likely continuing beyond the neutrally buoyant depth in both directions because of the need to overcome drag in the direction of travel.

Modeling energetic intake and daily energy budget

Overfishing or climate change-induced variation in the thermal structure of the water column may result in the need for deeper and/ or longer dives, which would further increase the metabolic cost of foraging. Thus, the thrust method used in the current study provides an opportunity to test how such changes in swimming kinematics translate to energy use, while broader methods such as the breathing frequency method only provide long-term estimates.

Estimating energetic expenditure for both diving and non-diving states using the thrust method allowed us to more accurately model the impact of varying prey capture rates, making it more useful (compared with the breathing frequency method) for modeling daily net energy budgets. As a part of this method, we had a series of variables (daily dive rate, prey wet weight, prey calorific content and prey captures per dive) that we could not measure directly for our CATS-tagged animals. Instead, we parameterized these variables as accurately as possible using our satellite tag and stomach content datasets as well as published literature. These values, while not

directly tied to the CATS-tagged animals, were generally sourced from the same geographic region, offering strong proxies for each metric. For instance, our average value for daily dive rate (\sim 35 dives day⁻¹) was sourced from 13 male animals tagged around the Hawaiian Islands, totaling ~176 days of on-animal data. These rates were similar to rates found previously for Hawaiian short-finned pilot whales (Baird et al., 2003), and were slightly lower than the dive rate that we estimated from Gm221116-J2 (\sim 53 dives day⁻¹). While not as robust, our value for prey wet weight was based on 341 squid beaks from 27 cephalopod prey species making up \sim 99% of the prey found within the stomach of a short-finned pilot whale stranded in Hawai'i. Our value of prey calorific content was based on non-Hawaiian data, instead using an average from eight cephalopod species across a range of body types (i.e. muscular, ammoniacal) across the Northeast Atlantic Ocean (Clarke et al., 1985). It is our hope that future work will increase the accuracy and precision of these parameters, as well as include additional variability among sex, age class and time of day.

Given our paucity of acoustic buzz data, we modeled the balance between energetic expenditure and intake for a range of per-dive prey capture rates sourced from the literature (Aguilar Soto et al., 2008; Shearer et al., 2022). This analysis did not allow us to definitively state whether short-finned pilot whales in Hawai'i are achieving a positive energetic balance outside of our limited daytime dataset, but it did allow us to offer a range of possible energetic scenarios and model minimum prey capture requirements.

Our results from this method (Fig. 7A) suggest that the average short-finned pilot whale in Hawai'i could maintain net energetic balance if they consume ~4 prey items per dive, a higher value than the average buzz rate from our small sample set of daytime dives with acoustic data (2.4±1.7 buzzes dive⁻¹). If we assume that our animals behave similarly to other island-associated short-finned pilot whales (Abecassis et al., 2015; Aguilar Soto et al., 2008; Alves et al., 2013; Baird et al., 2003), we might suspect that their buzz rates would be higher at night, resulting in these animals easily crossing into positive net energetic balance. If the similar diving behavior of island-associated pilot whales (Abecassis et al., 2015; Aguilar Soto et al., 2008; Alves et al., 2013; Baird et al., 2003) translates into similar daily values of energetic expenditure, we can assume that they might also have similar prey capture rate requirements to achieve a positive net energetic balance.

Annual and population-level energy requirements of Hawaiian short-finned pilot whales

If an individual captures enough prey to maintain a neutral net energetic balance, that translates into an average of $52,000\pm21,800$ squid whale⁻¹ year⁻¹ or 11.0 ± 5.00 tonnes of squid year⁻¹ (assuming an average wet weight of 210 ± 33.7 g squid⁻¹). Lockyer (1993) estimated the annual prey consumption of a 1000 kg long-finned pilot whales to be 11.3 tonnes year⁻¹. The short-finned pilot whales in our dataset were slightly smaller (~700 kg), suggesting that they may require slightly more energy on a permass basis.

The most recent abundance estimate of short-finned pilot whales in 2017 puts their population around ~8000 individuals in Hawaiian waters (Bradford et al., 2021). At this population, we can estimate the overall biomass of squid removed from the ecosystem at 88,000±37,000 tonnes year⁻¹. Bradford et al. (2021) also included abundance estimates from 2002 (~11,600) and 2010 (17,600). These values correspond with biomass removal estimates of 128,000±53,600 and 194,000±81,300 tonnes of squid year⁻¹, respectively. Squid typically display rapid life cycles (~1 year or

less) and high growth rates (Hoving and Robison, 2017; Jackson and O'Dor, 2001), positioning them as an abundant and reliable prey resource for short-finned pilot whales.

Unfortunately, the prey data in our current study is extremely limited, leaving open the possibility that less-abundant prey types might make up an important portion of the diet for short-finned pilot whales in Hawai'i. However, if future studies find similar results to ours, we might posit that the presence of such a readily available prey resource (squid) could explain the finding by Czapanskiy et al. (2021) that short-finned pilot whales are among the cetacean species most resilient to disturbance from loss of foraging opportunity – more so than both larger (e.g. sperm whale) and smaller (e.g. harbor porpoise) species. If short-finned pilot whales are, indeed, more resilient to foraging-related disturbance, it stands that their high rates of stranding (Hamilton, 2019; Parsons, 2017) do not result from a lack of prey availability.

Conclusions

Previous research has sought to estimate the energy budgets of wild cetacean populations using a variety of methods (e.g. breathing frequency, movement proxies, stroke counting), but our study is among the first to quantify energetic expenditure at a finer scale (e.g. between the low-expenditure descent and high-expenditure ascent phases of a foraging dive). Comparing the output of this thrust-based method against a simplified breathing frequency method, we found similar values for expenditure, especially for diving periods. Estimating field metabolic rates from breathing frequency is notably less complex in terms of data requirements and processing time, making it useful in cases where accelerometry tag or UAS-photogrammetry data are unavailable; however, further comparisons across various behavioral contexts are needed to truly understand the most effective applications for these and other methods of estimating energetic expenditure.

Utilizing the enhanced granularity of the thrust method, we were able to integrate multiple data streams and estimate the number of squid needed by short-finned pilot whales to maintain a neutral net energetic balance in Hawaiian waters. These results were slightly higher than the energy budget of the closely related long-finned pilot whale (Isojunno et al., 2018; Lockyer, 1993). And given that short-finned pilot whales in Hawai'i display broadly similar diving behavior to other island-associated cetacean populations (Aguilar Soto et al., 2008; Alves et al., 2013), we expect that our energetic estimates could apply to these other populations as well.

Model caveats

Our models provide a broadly useful framework for estimating the energetics of pilot whales and related species, but an important consideration in interpreting our results is the uncertainty introduced by a number of parameters. For instance, BMR is commonly estimated using allometric scaling relationships (e.g. the Kleiber curve), but these are unlikely to capture individual variability or physiological adaptations in deep-diving odontocetes such as pilot whales. Following on from BMR, we modeled HIF as a fixed proportion of BMR (15%), although HIF has been shown to vary with prey type, meal size, digestive efficiency, and feeding state (Smith et al., 1978). The metabolic-to-mechanical efficiency factor (u_{met}) is another variable that has been used in multiple studies across species (Fish, 1996; Gough et al., 2022; Potvin et al., 2021), but has not been validated in short-finned pilot whales or tested for variability with behavioral state in free-swimming animals. Our model also assumes a constant seawater density (1025 kg m⁻³), despite the fact that water density changes with temperature,

salinity, and depth – all of which can affect thrust power estimates used in calculating energetic costs. Additionally, our estimation of the thrust coefficient ($C_{\rm thrust}$) and propulsive efficiency ($\mu_{\rm prop}$) rely on modeled data from flapping foils (Chopra and Kambe, 1977) and kinematic parameters of the oscillatory tailbeat, such as angle of attack (α) and heave amplitude (h), that are difficult to directly measure in free-swimming animals using current biologging technology. We accounted for uncertainty in these parameters by incorporating $\pm 10\%$ variation, but the impact of precise swimming kinematics on hydrodynamic and energetic modeling remain a notable source of uncertainty.

Multiple respiration-related parameters used in the breathing frequency method (e.g. tidal volume, vital capacity, total lung capacity, oxygen extraction efficiency) are extremely difficult to measure in free-swimming animals, often necessitating the extrapolation of values from related species housed under human care. These variables are also likely to vary with behavior and exertion level, introducing additional layers of uncertainty in the estimation of field metabolic rate.

In addition to these physiological and environmental parameters, prey-related factors represent a significant source of uncertainty. Our estimates of prey energy density were based on literature values (Clarke et al., 1985), while prey mass estimates were based on a limited number of squid beaks recovered from a single stranded animal. Stomach content data from additional animals is sorely needed, as is a comprehensive overview of prey species and distribution throughout the short-finned pilot whale's Hawaiian habitat.

Future tag-based studies should aim for a more extensive dataset. with a goal of incorporating longer tag deployments, coverage for night-time hours, and targeted deployments on a variety of age and sex classes. Improving our estimates of daily foraging effort including both the number of dives per day and the number of prey captures per dive – requires greater temporal coverage across diel and seasonal cycles. Longer deployments would also improve our ability to quantify respiration patterns at the surface, which are critical for refining energetic estimates using the breathing frequency method. Likewise, additional high-resolution accelerometry data could support more granular estimates of thrust power output during diving, allowing us to better characterize variability in locomotor cost using the thrust method. These improvements would collectively enhance the robustness of our intake and expenditure estimates and enable greater inclusion of behavioral variation and environmental context into models of net energy intake.

Acknowledgements

We thank the staff and support crew at Pacific Whale Foundation for their logistical and field support during tag data collection efforts, and for providing analytical support and feedback on the manuscript. Thanks to the Cascadia Research Collective for providing their dataset of satellite tag deployments. We thank the members of the Marine Mammal Research Program at UH Manoa's Hawai'i Institute of Marine Biology for their substantial feedback on the structure and content of this work. We thank Dr Peter Madsen for his helpful feedback on the manuscript and figures. Finally, we thank Cameron Nemeth and Dr Kalikoaloha Martin for their help in drafting the Hawaiian language abstract for this manuscript. This paper represents HIMB and SOEST contribution numbers 2009 and 11991, respectively.

Competing interests

The authors declare no competing or financial interests.

Author contributions

Conceptualization: W.T.G., L.B.; Data curation: W.T.G., B.C.M., A.H., J.J.C., R.W.B., K.L.W., L.E., M.v.A., B.S.; Formal analysis: W.T.G., B.C.M., A.H., R.W.B., L.E., M.v.A., B.S., G.L.O.; Funding acquisition: R.W.B., K.L.W., A.P., S.H.S., L.B.; Investigation: W.T.G., B.C.M., A.H., J.J.C., R.W.B., K.L.W., L.E., M.v.A., B.S., A.P., G.L.O., S.H.S., L.B.; Methodology: W.T.G., B.C.M., A.H., A.M.B., L.B.; Project

administration: L.B.; Resources: J.J.C., R.W.B., K.L.W., A.P., S.H.S., W.A.W., L.B.; Software: W.T.G., B.C.M., A.H., L.E., M.v.A., A.M.B.; Visualization: W.T.G.; Writing – original draft: W.T.G., B.C.M., R.W.B., K.L.W., L.B.; Writing – review & editing: W.T.G., B.C.M., A.H., J.J.C., R.W.B., K.L.W., A.F., F.E.F., L.E., M.v.A., B.S., A.P., G.L.O., S.H.S., A.M.B., L.B.

Funding

This research was funded in part by grants from the Office of Naval Research (no. N00014-22-1-2721), the United States Pacific Fleet Environmental Readiness Division (no. W9126G2220033), NOAA Fisheries via the Cooperative Ecosystem Studies Unit (CESU) award NA19NMF4720181, and the DoD's Defense University Research Instrumentation Program (N00014-19-1-2612 and N00014-21-1-2249). Stomach content collection and analysis was funded by the Office of Naval Research (no. N00014-17-1-2789) and with support of the NOAA National Marine Fisheries Service Johan H. Prescott Marine Mammal Rescue Assistance Grant Program. Satellite tagging field efforts performed by Cascadia Research Collective were supported by multiple sources, including: the Office of Naval Research, United States Navy Living Marine Resources, United States Navy Pacific Fleet, the NOAA Pacific Islands Fisheries Science Center, and a NOAA Species Recovery Grant. Additional funding was provided by the members and supporters of Pacific Whale Foundation and by the Omidyar Ohana Foundation.

Data and resource availability

Data related to the analyses in this study can be found at Data Dryad (DOI: https://doi.org/10.5061/dryad.8gtht7720) or at https://github.com/wgough/ HawaiiPilotWhaleEnergetics. For more information, please contact the authors. All relevant data and details of resources can be found within the article and its supplementary information.

References

- Abecassis, M., Polovina, J., Baird, R. W., Copeland, A., Drazen, J. C., Domokos, R., Oleson, E., Jia, Y., Schorr, G. S., Webster, D. L. et al. (2015). Characterizing a foraging hotspot for short-finned pilot whales and blainville's beaked whales located off the west side of hawai'i island by using tagging and oceanographic data. *PLoS ONE* 10, e0142628. doi:10.1371/journal.pone.0142628
- Aguilar Soto, N., Johnson, M. P., Madsen, P. T., Díaz, F., Domínguez, I., Brito, A. and Tyack, P. L. (2008). Cheetahs of the deep sea: deep foraging sprints in short-finned pilot whales off Tenerife (Canary Islands). *J. Anim. Ecol.* 77, 936-947. doi:10.1111/j.1365-2656.2008.01393.x
- Allen, A. S., Read, A. J., Shorter, K. A., Gabaldon, J., Blawas, A. M., Rocho-Levine, J. and Fahlman, A. (2022). Dynamic body acceleration as a proxy to predict the cost of locomotion in bottlenose dolphins. *J. Exp. Biol.* **225**, jeb243121. doi:10.1242/jeb.243121
- Alves, F., Dinis, A., Ribeiro, C., Nicolau, C., Kaufmann, M., Fortuna, C. M. and Freitas, L. (2013). Daytime dive characteristics from six short-finned pilot whales *Globicephala macrorhynchus* off Madeira Island. *Arquipélago. Life Mar. Sci.* 31, 106-121. doi:10.1111/mms.12137
- Alves, F., Mesnick, S. L., Rosso, M. and Pitman, R. L. (2023). Beaked Whale Sexual Dimorphism, Mating Strategies, and Diversification. In Sex in Cetaceans: Morphology, Behavior, and the Evolution of Sexual Strategies (ed. B. Würsig and D. N. Orbach), pp. 385-413. Cham: Springer International Publishing.
- Aoki, K., Amano, M., Yoshioka, M., Mori, K., Tokuda, D. and Miyazaki, N. (2007). Diel diving behavior of sperm whales off Japan. *Mar. Ecol. Prog. Ser.* **349**, 277-287. doi:10.3354/meps07068
- Aoki, K., Watanabe, Y. Y., Crocker, D. E., Robinson, P. W., Biuw, M., Costa, D. P., Miyazaki, N., Fedak, M. A. and Miller, P. J. O. (2011). Northern elephant seals adjust gliding and stroking patterns with changes in buoyancy: validation of at-sea metrics of body density. *J. Exp. Biol.* 214, 2973-2987. doi:10.1242/jeb. 055137
- Aoki, K., Amano, M., Mori, K., Kourogi, A., Kubodera, T. and Miyazaki, N. (2012).
 Active hunting by deep-diving sperm whales: 3D dive profiles and maneuvers during bursts of speed. *Mar. Ecol. Prog. Ser.* 444, 289-301. doi:10.3354/meps09371
- Aoki, K., Sato, K., Isojunno, S., Narazaki, T. and Miller, P. J. O. (2017). High diving metabolic rate indicated by high-speed transit to depth in negatively buoyant long-finned pilot whales. *J. Exp. Biol.* **220**, 3802-3811. doi:10.1242/jeb.158287
- Arranz, P., DeRuiter, S. L., Stimpert, A. K., Neves, S., Friedlaender, A. S., Goldbogen, J. A., Visser, F., Calambokidis, J., Southall, B. L. and Tyack, P. L. (2016). Discrimination of fast click-series produced by tagged Risso's dolphins (*Grampus griseus*) for echolocation or communication. *J. Exp. Biol.* 219, 2898-2907. doi:10.1242/jeb.144295
- Arranz, P., Benoit-Bird, K. J., Friedlaender, A. S., Hazen, E. L., Goldbogen, J. A., Stimpert, A. K., Deruiter, S. L., Calambokidis, J., Southall, B. L., Fahlman, A. et al. (2019). Diving behavior and fine-scale kinematics of free-ranging Risso's Dolphins foraging in shallow and deep-water habitats. *Front. Ecol. Evol.* 7, 53. doi:10.3389/fevo.2019.00053

- Arranz, P., Christiansen, F., Glarou, M., Gero, S., Visser, F., Oudejans, M. G., Aguilar De Soto, N. and Sprogis, K. (2022). Body condition and allometry of free-ranging short-finned pilot whales in the North Atlantic. Sustainability 14, 14787. doi:10.3390/su142214787
- **Bainbridge, R.** (1958). The speed of swimming of fish as related to size and to the frequency and amplitude of the tail beat. *J. Exp. Biol.* **35**, 109-133. doi:10.1242/ieb.35.1.109
- Baird, R. W. (2016). The Lives of Hawai'i's Dolphins and Whales: Natural History and Conservation. University of Hawaii Press.
- Baird, R. W., McSweeney, D. J., Heithaus, M. R. and Marshall, G. J. (2003). Short-finned pilot whale diving behavior: deep feeders and day-time socialites. In Abstracts, Fifteenth Biennial Conference on the Biology of Marine Mammals, pp. 14-19
- Barrett, D. S., Triantafyllou, M. S., Yue, D. K. P., Grosenbaugh, M. A. and Wolfgang, M. J. (1999). Drag reduction in fish-like locomotion. *J. Fluid Mech.* 392, 183-212. doi:10.1017/S0022112099005455
- Beasley, I., Cherel, Y., Robinson, S., Betty, E., Hagihara, R. and Gales, R. (2019). Stomach contents of long-finned pilot whales, *Globicephala melas* mass-stranded in Tasmania. *PLoS ONE* 14, e0206747. doi:10.1371/journal.pone.0206747
- Blawas, A. M. (2025). respdetect: A Matlab tool for detecting breath events from whale biologger data. *J. Open Source Software* 10, 7858.
- Bose, N., Lien, J. and Ahia, J. (1990). Measurements of the bodies and flukes of several cetacean species. Proc. R. Soc. B Biol. Sci. 242, 163-173. doi:10.1098/ rspb 1990 0120
- **Boyd, I. L.** (1997). The behavioural and physiological ecology of diving. *Trends Ecol. Evol.* **12**, 213-217. doi:10.1016/S0169-5347(97)01054-9
- Boyd, I. L. and Hoelzel, A. R. (2002). Energetics: Consequences for fitness. In Marine Mammal Biology: An Evolutionary Approach. Blackwell Science Ltd.
- Bradford, A. L., Oleson, E. M., Forney, K. A., Moore, J. E. and Barlow, J. (2021). Line-transect Abundance Estimates of Cetaceans in U.S. Waters around the Hawaiian Islands in 2002, 2010, and 2017. doi:10.25923/daz4-kw84
- Cade, D. E., Barr, K. R., Calambokidis, J., Friedlaender, A. S. and Goldbogen, J. A. (2018). Determining forward speed from accelerometer jiggle in aquatic environments. J. Exp. Biol. 221, jeb170449.
- Cade, D. E., Gough, W. T., Czapańskiy, M. F., Fahlbusch, J. A., Kahane-Rapport, S. R., Linsky, J. M. J., Nichols, R. C., Oestreich, W. K., Wisniewska, D. M., Friedlaender, A. S. et al. (2021). Tools for integrating inertial sensor data with video bio-loggers, including estimation of animal orientation, motion, and position. *Anim. Biotelemetry* 9, 34. doi:10.1186/s40317-021-00256-w
- Carretta, J. V., Oleson, E. M., Forney, K. A., Bradford, A. L., Yano, K., Weller, D. W., Lang, A. R., Baker, J., Orr, A. J., Hanson, B. et al. (2023). *Draft U.S. Pacific Marine Mammal Stock Assessments:* 2023. NOAA.
- Chimienti, M., Desforges, J.-P., Beumer, L. T., Nabe-Nielsen, J., Van Beest, F. M. and Schmidt, N. M. (2020). Energetics as common currency for integrating high resolution activity patterns into dynamic energy budget-individual based models. *Ecol. Model.* 434, 109250. doi:10.1016/j.ecolmodel.2020.109250
- Chopra, M. G. and Kambe, T. (1977). Hydromechanics of lunate-tail swimming propulsion. Part 2. J. Fluid Mech. 79, 49-69. doi:10.1017/S0022112077000032
- Christiansen, F., Dujon, A. M., Sprogis, K. R., Arnould, J. P. Y. and Bejder, L. (2016). Noninvasive unmanned aerial vehicle provides estimates of the energetic cost of reproduction in humpback whales. *Ecosphere* 7, e01468. doi:10.1002/ ecs2.1468
- Christiansen, F., Vivier, F., Charlton, C., Ward, R., Amerson, A., Burnell, S. and Bejder, L. (2018). Maternal body size and condition determine calf growth rates in southern right whales. *Mar. Ecol. Prog. Ser.* **592**, 267-281. doi:10.3354/meps12522
- Christiansen, F., Sprogis, K. R., Nielsen, M. L. K., Glarou, M. and Bejder, L. (2023).
 Energy expenditure of southern right whales varies with body size, reproductive state and activity level. J. Exp. Biol. 226, jeb245137. doi:10.1242/jeb.245137
- Clarke, A., Clarke, M. R., Holmes, L. J. and Waters, T. D. (1985). Calorific Values and Elemental Analysis of Eleven Species of Oceanic Squids (Mollusca: Cephalopoda). J. Mar. Biol. Ass. 65, 983-986. doi:10.1017/S0025315400019457
- Clarke, M. R., Martins, H. R. and Pascoe, P. (1997). The diet of sperm whales (*Physeter macrocephalus* linnaeus 1758) off the azores. *Philos. Trans. R. Soc. Lond. Ser. B Biol. Sci.* **339**, 67-82. doi:10.1098/rstb.1993.0005
- Cole, M. R., Ware, C., McHuron, E. A., Costa, D. P., Ponganis, P. J. and McDonald, B. I. (2023). Deep dives and high tissue density increase mean dive costs in California sea lions (*Zalophus californianus*). J. Exp. Biol. 226, ieb246059. doi:10.1242/ieb.246059
- Cooke, J. and Klinowska, M. (1991). Dolphins, Porpoises and Whales of the World: The IUCN Red Data Book. IUCN.
- Crossin, G. T., Cooke, S. J., Goldbogen, J. A. and Phillips, R. A. (2014). Tracking fitness in marine vertebrates: current knowledge and opportunities for future research. *Mar. Ecol. Prog. Ser.* 496, 1-17. doi:10.3354/meps10691
- Curren, K. C. (1992). Designs for swimming: morphometrics and swimming dynamics of several cetacean species. MSc thesis, Memorial University of Newfoundland, St John's, Newfoundland, Canada.
- Czapanskiy, M. F., Savoca, M. S., Gough, W. T., Segre, P. S., Wisniewska, D. M., Cade, D. E. and Goldbogen, J. A. (2021). Modelling short-term energetic costs of sonar disturbance to cetaceans using high-resolution foraging data. *J. Appl. Ecol.* 58, 1643-1657. doi:10.1111/1365-2664.13903

- Davis, R. W., Fiori, L., Würsig, B. and Orbach, D. N. (2024). Drag reduction and locomotory power in dolphins: Gray's paradox revealed. J. R. Soc. Interface 21, 20240227. doi:10.1098/rsif.2024.0227
- Dawson, S. M., Bowman, M. H., Leunissen, E. and Sirguey, P. (2017). Inexpensive aerial photogrammetry for studies of whales and large marine animals. Front. Mar. Sci. 4, 366. doi:10.3389/fmars.2017.00366
- Demas, G. and Nelson, R. (2012). Ecoimmunology. Oxford University Press.
- Eguiguren, A., Konrad Clarke, C. M. and Cantor, M. (2023). Sperm whale reproductive strategies: current knowledge and future directions. In Sex in Cetaceans: Morphology, Behavior, and the Evolution of Sexual Strategies (ed. B. Würsig and D. N. Orbach), pp. 443-467. Cham: Springer International Publishing.
- Evans, K. and Hindell, M. A. (2004a). The diet of sperm whales (*Physeter macrocephalus*) in southern Australian waters. *ICES J. Mar. Sci.* **61**, 1313-1329. doi:10.1016/j.icesjms.2004.07.026
- Evans, K. and Hindell, M. A. (2004b). The age structure and growth of female sperm whales (*Physeter macrocephalus*) in southern Australian waters. *J. Zool.* **263**, 237-250. doi:10.1017/S0952836904005096
- Fahlman, A., Loring, S. H., Ferrigno, M., Moore, C., Early, G., Niemeyer, M., Lentell, B., Wenzel, F., Joy, R. and Moore, M. J. (2011). Static inflation and deflation pressure–volume curves from excised lungs of marine mammals. *J. Exp. Biol.* 214, 3822. doi:10.1242/jeb.056366
- Fahlman, A., Van Der Hoop, J., Moore, M. J., Levine, G., Rocho-Levine, J. and Brodsky, M. (2016). Estimating energetics in cetaceans from respiratory frequency: why we need to understand physiology. *Biol. Open* 5, 436-442. doi:10. 1242/bio.017251
- Fahlman, A., Moore, M. J. and Garcia-Parraga, D. (2017). Respiratory function and mechanics in pinnipeds and cetaceans. J. Exp. Biol. 220, 1761-1773. doi:10. 1242/jeb.126870
- Fahlman, A., Allen, A. S., Blawas, A., Sweeney, J., Stone, R., Trainor, R. F., Jensen, F. H., McHugh, K., Allen, J. B., Barleycorn, A. A. et al. (2023). Surface and diving metabolic rates, and dynamic aerobic dive limits (dADL) in near-and off-shore bottlenose dolphins, Tursiops spp., indicate that deep diving is energetically cheap. *Mar. Mamm. Sci.* 39, 976-993. doi:10.1111/mms.13023
- Fahlman, A., Schorr, G. S., Sweeney, D. A., Rone, B. K., Coates, S. N., Allen, A. S., Martín López, L. M., Jarvis, S. M. and Falcone, E. A. (2025). Modelling the effect of varying metabolic rate and cardiac output on estimated tissue and blood O2 and CO2 levels in an extreme deep-diver, the goose-beaked whale (*Ziphius cavirostris*). Exp. Physiol. 108, 1100-1112. doi:10.1113/EP093021
- Farmer, N. A., Noren, D. P., Fougères, E. M., Machernis, A. and Baker, K. (2018). Resilience of the endangered sperm whale *Physeter macrocephalus* to foraging disturbance in the Gulf of Mexico, USA: a bioenergetic approach. *Mar. Ecol. Prog. Ser.* 589, 241-261, doi:10.3354/meps12457
- Feyrer, L. J., Zhao, S. T., Whitehead, H. and Matthews, C. J. D. (2020). Prolonged maternal investment in northern bottlenose whales alters our understanding of beaked whale reproductive life history. PLoS ONE 15, e0235114. doi:10.1371/journal.pone.0235114
- Fish, F. E. (1993). Power output and propulsive efficiency of swimming bottlenose dolphins (Tursiops truncatus). *J. Exp. Biol.* **185**, 179-183. doi:10.1242/jeb.185.1.179
- Fish, F. E. (1996). Transitions from drag-based to lift-based propulsion in mammalian swimming. *Am. Zool.* **36**, 628-641. doi:10.1093/icb/36.6.628
- **Fish, F. E.** (1998). Comparative kinematics and hydrodynamics of odontocete cetaceans: morphological and ecological correlates with swimming performance. *J. Exp. Biol.* **201**, 2867-2877. doi:10.1242/jeb.201.20.2867
- Fish, F. E. (2006). The myth and reality of Gray's paradox: implication of dolphin drag reduction for technology. *Bioinspir. Biomim.* 1, R17-R25. doi:10.1088/1748-3182/1/2/R01
- Fish, F. E., Legac, P., Williams, T. M. and Wei, T. (2014). Measurement of hydrodynamic force generation by swimming dolphins using bubble DPIV. *J. Exp. Biol.* 217, 252-260. doi:10.1242/jeb.087924
- Friedlaender, A. S., Hazen, E. L., Nowacek, D. P., Halpin, P. N., Ware, C., Weinrich, M. T., Hurst, T. and Wiley, D. (2009). Diel changes in humpback whale *Megaptera novaeangliae* feeding behavior in response to sand lance Ammodytes spp. behavior and distribution. *Mar. Ecol. Prog. Ser.* 395, 91-100. doi:10.3354/meps08003
- Gabaldon, J. T., Zhang, D., Rocho-Levine, J., Moore, M. J., Van Der Hoop, J., Barton, K. and Shorter, K. A. (2022). Tag-based estimates of bottlenose dolphin swimming behavior and energetics. J. Exp. Biol. 225, jeb244599. doi:10.1242/jeb. 244599
- Gaskin, D. E. and Cawthorn, M. W. (1967). Diet and feeding habits of the sperm whale (*Physeter Catodon L.*) in the cook strait region of New Zealand. N. Z. J. Mar. Freshw. Res. 1, 156-179. doi:10.1080/00288330.1967.9515201
- Glarou, M., Gero, S., Frantzis, A., Brotons, J. M., Vivier, F., Alexiadou, P., Cerdà, M., Pirotta, E. and Christiansen, F. (2023). Estimating body mass of sperm whales from aerial photographs. *Mar. Mamm. Sci.* **39**, 251-273. doi:10.1111/mms. 12982
- Goldbogen, J. A., Cade, D. E., Wisniewska, D. M., Potvin, J., Segre, P. S., Savoca, M. S., Hazen, E. L., Czapanskiy, M. F., Kahane-Rapport, S. R., DeRuiter, S. L. et al. (2019). Why whales are big but not bigger: Physiological drivers and ecological limits in the age of ocean giants. *Science* 366, 1367-1372. doi:10.1126/science.aax9044

- Gómez-Villota, F. (2007). Sperm whale diet in New Zealand. MSc thesis, University of Auckland. Auckland. New Zealand.
- Gough, W. T., Segre, P. S., Bierlich, K. C., Cade, D. E., Potvin, J., Fish, F. E., Dale, J., Di Clemente, J., Friedlaender, A. S., Johnston, D. W. et al. (2019). Scaling of swimming performance in baleen whales. *J. Exp. Biol.* 222, jeb204172. doi:10.1242/ieb.204172
- Gough, W. T., Smith, H. J., Savoca, M. S., Czapanskiy, M. F., Fish, F. E., Potvin, J., Bierlich, K. C., Cade, D. E., Di Clemente, J., Kennedy, J. et al. (2021). Scaling of oscillatory kinematics and Froude efficiency in baleen whales. *J. Exp. Biol.* 224, jeb237586. doi:10.1242/jeb.237586
- Gough, W. T., Cade, D. E., Czapańskiy, M. F., Potvin, J., Fish, F. E., Kahane-Rapport, S. R., Savoca, M. S., Bierlich, K. C., Johnston, D. W., Friedlaender, A. S. et al. (2022). Fast and furious: energetic tradeoffs and scaling of high-speed foraging in Rorqual Whales. *Integr. Org. Biol.* 4, obac038. doi:10.1093/iob/obac038
- Gray, J. (1936). Studies in animal locomotion: VI. The propulsive powers of the dolphin. J. Exp. Biol. 13, 192-199. doi:10.1242/jeb.13.2.192
- Hamilton, L. J. (2019). Large mass strandings of selected odontocete species: statistics, locations, and relation to earth processes. J. Cetacean Res. Manag. 19, 57-78. doi:10.47536/jcrm.v19i1.415
- Hernández-Garciá, V. and Martín, V. (1994). Stomach contents of two short-finned pilot whale (*Globicephala macrorhynchus* gray, 1846) (Cetacea, Delphinidae) off the Canary Islands: a preliminary note. *International Council for the Exploration of the Sea* 1-9
- Hin, V., Harwood, J. and de Roos, A. M. (2019). Bio-energetic modeling of medium-sized cetaceans shows high sensitivity to disturbance in seasons of low resource supply. Ecol. Appl. 29, e01903. doi:10.1002/eap.1903
- Hin, V., de Roos, A. M., Benoit-Bird, K. J., Claridge, D. E., DiMarzio, N., Durban, J. W., Falcone, E. A., Jacobson, E. K., Jones-Todd, C. M., Pirotta, E. et al. (2023). Using individual-based bioenergetic models to predict the aggregate effects of disturbance on populations: A case study with beaked whales and Navy sonar. PLoS ONE 18, e0290819. doi:10.1371/journal.pone.0290819
- Hohn, A. A., Rotstein, D. S., Harms, C. A. and Southall, B. L. (2006). Report on Marine Mammal Unusual Mortality Event UMESE0501Sp: Multispecies Mass Stranding of Pilot Whales (Globicephala macrorhynchus), Minke Whale (Balaenoptera acutorostrata), and Dwarf Sperm Whales (Kogia sima) in North Carolina on 15-16 January 2005. Beaufort, NC: NOAA/National Marine Fisheries Service/Southeast Fisheries Science Center.
- Hooker, S. K., Baird, R. W. and Fahlman, A. (2009). Could beaked whales get the bends? Respir. Physiol. Neurobiol. 167, 235-246. doi:10.1016/j.resp.2009. 04.023
- Hoving, H. J. T. and Robison, B. H. (2017). The pace of life in deep-dwelling squids. *Deep Sea Res. Part I Oceanogr. Res. Papers* **126**, 40-49. doi:10.1016/j. dsr.2017.05.005
- Irvine, L., Palacios, D. M., Urbán, J. and Mate, B. (2017). Sperm whale dive behavior characteristics derived from intermediate-duration archival tag data. *Ecol. Evol.* 7, 7822-7837, doi:10.1002/ece3.3322
- Isojunno, S., Aoki, K., Curé, C., Kvadsheim, P. H. and Miller, P. J. O. M. (2018). Breathing patterns indicate cost of exercise during diving and response to experimental sound exposures in long-finned pilot whales. *Front. Physiol.* 9, 1462. doi:10.3389/fphys.2018.01462
- Jackson, G. and O'Dor, R. K. (2001). Time, space and the ecophysiology of squid growth, life in the fast lane. Vie Milieu 51, 205-215.
- Johnson, M., Madsen, P. T., Zimmer, W. M. X., Aguilar de Soto, N. and Tyack, P. L. (2004). Beaked whales echolocate on prey. Proc. R. Soc. B 271 Suppl. 6, S386-S386. doi:10.1098/rsbl.2004.0208
- Johnson, M., Madsen, P., Tyack, P. and Aguilar De Soto, N. (2005). A binaural acoustic recording tag reveals details of deep foraging in beaked whales. *J. Acoust. Soc. Am.* 117, 2524-2524. doi:10.1121/1.4809422
- Johnson, M., Madsen, P. T., Zimmer, W. M. X., Aguilar de Soto, N. and Tyack, P. L. (2006). Foraging Blainville's beaked whales (*Mesoplodon densirostris*) produce distinct click types matched to different phases of echolocation. *J. Exp. Biol.* 209, 5038-5050. doi:10.1242/jeb.02596
- Kasuya, T. (1977). Age determination and growth of the Baird's beaked whale with a comment on the fetal growth rate. Scientific Reports of the Whales Research Institute, 1-20.
- Kasuya, T. (1991). Density dependent growth in north pacific sperm whales. *Mar. Mamm. Sci.* 7, 230-257. doi:10.1111/j.1748-7692.1991.tb00100.x
- Mamm. Sci. 7, 230-257. doi:10.1111/j.1748-7692.1991.tb00100.x **Kasuya, T. and Matsui, S.** (1984). Age determination and growth of the short-finned
- pilot whale off the pacific coast of japan. *Sci. Rep. Whales Res. Inst.* **35**, 57-91. **Kebke, A., Samarra, F. and Derous, D.** (2022). Climate change and cetacean health: impacts and future directions. *Philos. Trans. R. Soc. B Biol. Sci.* **377**, 20210249. doi:10.1098/rstb.2021.0249
- Kleiber, M. (1975). Metabolic turnover rate: a physiological meaning of the metabolic rate per unit body weight. J. Theor. Biol. 53, 199-204. doi:10.1016/ 0022-5193(75)90110-1
- Kooyman, G. L. (1973). Respiratory Adaptations in Marine Mammals. Am. Zool. 13, 457-468. doi:10.1093/icb/13.2.457
- Kramer, M. O. (1961). The Dolphins' Secret. J. Am. Soc. Naval Eng. 73, 103-108. doi:10.1111/j.1559-3584.1961.tb02422.x

- Kramer, M. O. (1962). Boundary layer stabilization by distributed damping. *Nav. Eng. J.* 74, 341-348. doi:10.1111/j.1559-3584.1962.tb05568.x
- **Krogh, A.** (1934). Physiology of the blue whale. *Nature* **133**, 635-637. doi:10.1038/133635a0
- Kvadsheim, P. H., Miller, P. J. O., Tyack, P. L., Sivle, L. D., Lam, F. P. A. and Fahlman, A. (2012). Estimated tissue and blood N(2) levels and risk of decompression sickness in deep-, intermediate-, and shallow-diving toothed whales during exposure to naval sonar. *Front. Physiol.* 3, 125. doi:10.3389/fphys. 2012.00125
- Lighthill, M. J. (1971). Large-amplitude elongated-body theory of fish locomotion. *Proc. R. Soc. B* **179**, 125-138. doi:10.1098/rspb.1971.0085
- Lockyer, C. (1981). Growth and energy budgets of large baleen whales from the Southern Hemisphere. In Mammals in the Seas: Vol. III, General Papers and Large Cetaceans. FAO Fisheries Series No. 5, pp. 379-487.
- **Lockyer, C.** (1993). Seasonal changes in body fat condition of northeast Atlantic pilot whales, and their biological significance. *Report of the International Whaling Commission* (Special Issue) **14**: 324-350.
- Luna, A., Escánez, A., Marrero, J., Íñiguez, E., Pérez, J. A. and Sánchez, P. (2024). Early prey intake of a short–finned pilot whale (*Globicephala macrorhynchus* Gray, 1846, Cetacea: Delphinidae) in the Canary Islands. *Ecol. Evol.* 14, e11139. doi:10.1002/ece3.11139
- MacLeod, C. D. (2005). How big is a beaked whale? A review of body length and sexual size dimorphism in the family Ziphiidae. J. Cetacean Res. Manage. 7, 301-308. doi:10.47536/icrm.v7i3.739
- MacLeod, C. D. (2018). Beaked Whales, Overview. In Encyclopedia of Marine Mammals (Third Edition) (ed. B. Würsig, J. G. M. Thewissen, and K. M. Kovacs), pp. 80-83. Academic Press.
- MacLeod, C., Santos, M., López, A. and Pierce, G. (2006). Relative prey size consumption in toothed whales: implications for prey selection and level of specialisation. *Mar. Ecol. Prog. Ser.* 326, 295-307. doi:10.3354/meps326295
- Madsen, P. T., Johnson, M., Aguilar de Soto, N., Zimmer, W. M. X. and Tyack, P. (2005). Biosonar performance of foraging beaked whales (*Mesoplodon densirostris*). J. Exp. Biol. 208, 181-194. doi:10.1242/jeb.01327
- Mahaffy, S. D., Baird, R. W., McSweeney, D. J., Webster, D. L. and Schorr, G. S. (2015). High site fidelity, strong associations, and long-term bonds: short-finned pilot whales off the island of Hawai'i. *Mar. Mamm. Sci.* 31, 1427-1451. doi:10. 1111/mms.12234
- Martin, L. B., Weil, Z. M. and Nelson, R. J. (2008). Seasonal changes in vertebrate immune activity: mediation by physiological trade-offs. *Phil. Trans. R. Soc. B* 363, 321-339. doi:10.1098/rstb.2007.2142
- Martin López, L. M., Miller, P. J. O., Aguilar De Soto, N. and Johnson, M. (2015).
 Gait switches in deep-diving beaked whales: biomechanical strategies for long-duration dives. J. Exp. Biol. 218, 1325-1338. doi:10.1242/jeb.106013
- Massaad, F., Lejeune, T. M. and Detrembleur, C. (2007). The up and down bobbing of human walking: a compromise between muscle work and efficiency. J. Physiol. 582, 789-799. doi:10.1113/jphysiol.2007.127969
- McComb-Turbitt, S., Costa, J., Whitehead, H. and Auger-Méthé, M. (2021). Small-scale spatial distributions of long-finned pilot whales change over time, but foraging hot spots are consistent: Significance for marine wildlife tourism management. Mar. Mamm. Sci. 37, 1196-1211. doi:10.1111/mms.12821
- Mercer, M. C. (1975). Modified Leslie–DeLury Population Models of the Long-Finned Pilot Whale (*Globicephala melaena*) and Annual Production of the Short-Finned Squid (Illex illecebrosus) Based upon their Interaction at Newfoundland. *J. Fish. Res. Bd. Can.* 32, 1145-1154. doi:10.1139/f75-135
- Meyer, C. E., Zaeschmar, J. R. and Constantine, R. (2024). Occurrence, site-fidelity and photo-identification of long-finned pilot whales in Aotearoa New Zealand. N. Z. J. Mar. Freshw. Res. 0, 1-20.
- Miller, P. J. O., Johnson, M. P., Tyack, P. L. and Terray, E. A. (2004a). Swimming gaits, passive drag and buoyancy of diving sperm whales Physeter macrocephalus. *J. Exp. Biol.* **207**, 1953-1967. doi:10.1242/jeb.00993
- Miller, P. J. O., Johnson, M. and Tyack, P. L. (2004b). Sperm whale behaviour indicates the use of echolocation click buzzes "creaks" in prey capture. *Proc. R. Soc. B* 271, 2239-2247. doi:10.1098/rspb.2004.2863
- Miller, P. J. O., Biuw, M., Watanabe, Y. Y., Thompson, D. and Fedak, M. A. (2012). Sink fast and swim harder! Round-trip cost-of-transport for buoyant divers. *J. Exp. Biol.* 215, 3622-3630. doi:10.1242/jeb.070128
- Miller, B. S., Growcott, A., Slooten, E. and Dawson, S. M. (2013). Acoustically derived growth rates of sperm whales (*Physeter macrocephalus*) in Kaikoura, New Zealand. J. Acoust. Soc. Am. 134, 2438-2445. doi:10.1121/1.4816564
- Minton, G., Reeves, R. and Braulik, G. (2018b). IUCN Red List of Threatened Species: Globicephala melas. IUCN Red List of Threatened Species 2019, e.T9250A50356171. doi:10.2305/IUCN.UK.20182.RLTS.T9250A50356171.en
- Minton, G., Braulik, G. and Reeves, R. (2018a). IUCN Red List of Threatened Species: Globicephala macrorhynchus. IUCN Red List of Threatened Species 2019, e.T9249A50355227. doi:10.2305/IUCN.UK.20182.RLTS. T9249A50355227.en
- Mintzer, V. J., Gannon, D. P., Barros, N. B. and Read, A. J. (2008). Stomach contents of mass–stranded short–finned pilot whales (*Globicephala macrorhynchus*) from North Carolina. *Mar. Mamm. Sci.* **24**, 290-302. doi:10. 1111/j.1748-7692.2008.00189.x

- Narazaki, T., Isojunno, S., Nowacek, D. P., Swift, R., Friedlaender, A. S., Ramp, C., Smout, S., Aoki, K., Deecke, V. B., Sato, K. et al. (2018). Body density of humpback whales (*Megaptera novaengliae*) in feeding aggregations estimated from hydrodynamic gliding performance. *PLoS ONE* 13, e0200287. doi:10.1371/journal.pone.0200287
- Nazario, E. C., Cade, D. E., Bierlich, K. C., Czapanskiy, M. F., Goldbogen, J. A., Kahane-Rapport, S. R., Van Der Hoop, J. M., San Luis, M. T. and Friedlaender, A. S. (2022). Baleen whale inhalation variability revealed using animal-borne video tags. *PeerJ* 10, e13724-e13724. doi:10.7717/peerj.13724
- New, L. F., Moretti, D. J., Hooker, S. K., Costa, D. P. and Simmons, S. E. (2013).
 Using Energetic Models to Investigate the Survival and Reproduction of Beaked Whales (family Ziphiidae). PLoS ONE 8, e68725. doi:10.1371/journal.pone.0068725
- Nishiwaki, M., Ohsumi, S. and Maeda, Y. (1963). Change of form in the sperm whale accompanied with growth. *Sci.entific Rep. Whales Res. Inst. Tokyo* 17, 1-17.
- Noren, S. R. and Williams, T. M. (2000). Body size and skeletal muscle myoglobin of cetaceans: adaptations for maximizing dive duration. *Comp. Biochem. Physiol. A Mol. Integr. Physiol.* **126**, 181-191. doi:10.1016/S1095-6433(00)00182-3
- Ohsumi, S. (1965). Reproduction of the sperm whale in the north-west pacific. Sci. Rep. Whales Res. Inst. Tokyo 19, 1-35.
- Overholtz, W. J. and Gordon, W. T. (1991). Diet composition of pilot whales *Globicephala sp.* and common dolphins *Delphinus delphis* in the Mid-Atlantic Bight during spring 1989. *Fish. Bull.* **89**, 723-728.
- Owen, K., Andrews, R. D., Baird, R. W., Schorr, G. S. and Webster, D. L. (2019). Lunar cycles influence the diving behavior and habitat use of short-finned pilot whales around the main Hawaiian Islands. *Mar. Ecol. Prog. Ser.* **629**, 193-206. doi:10.3354/meps13123
- Pabst, D. A., McLellan, W. A. and Rommel, S. A. (2016). How to Build a Deep Diver: The Extreme Morphology of Mesoplodonts. *Integr. Comp. Biol.* 56, 1337-1348. doi:10.1093/icb/icw126
- Parry, D. A. (1949). The swimming of whales and a discussion of Gray's paradox. J. Exp. Biol. 26, 24-28. doi:10.1242/jeb.26.1.24
- Parsons, E. C. M. (2017). Impacts of navy sonar on whales and dolphins: now beyond a smoking gun? Front. Mar. Sci. 4, 295. doi:10.3389/fmars.2017.00295
- Pedersen, M. B., Tønnesen, P., Malinka, C. E., Ladegaard, M., Johnson, M., Aguilar De Soto, N. and Madsen, P. T. (2021). Echolocation click parameters of short-finned pilot whales (*Globicephala macrorhynchus*) in the wild. *J. Acoust.* Soc. Am. 149, 1923-1931. doi:10.1121/10.0003762
- Potvin, J., Cade, D. E., Werth, A. J., Shadwick, R. E. and Goldbogen, J. A. (2021). Rorqual lunge-feeding energetics near and away from the kinematic threshold of optimal efficiency. *Integr. Org. Biol.* 3. doi:10.1093/iob/obab005
- Quick, N. J., Isojunno, S., Sadykova, D., Bowers, M., Nowacek, D. P. and Read, A. J. (2017a). Hidden Markov models reveal complexity in the diving behaviour of short-finned pilot whales. Sci. Rep. 7, 45765. doi:10.1038/srep45765
- Quick, N., Scott-Hayward, L., Sadykova, D., Nowacek, D. and Read, A. (2017b).
 Effects of a scientific echo sounder on the behavior of short-finned pilot whales
 (Globicephala macrorhynchus). Can. J. Fish. Aquat. Sci. 74, 716-726. doi:10.
 1139/cjfas-2016-0293
- Quick, N. J., Cioffi, W. R., Shearer, J. M., Fahlman, A. and Read, A. J. (2020). Extreme diving in mammals: first estimates of behavioural aerobic dive limits in Cuvier's beaked whales. J. Exp. Biol. 223, jeb222109. doi:10.1242/jeb. 222109
- Rechsteiner, E. U., Rosen, D. A. S. and Trites, A. W. (2013). Energy requirements of Pacific white-sided dolphins (*Lagenorhynchus obliquidens*) as predicted by a bioenergetic model. *J. Mammal.* 94, 820-832. doi:10.1644/12-MAMM-A-206.1
- Ridgway, S. (1986). Diving by Cetaceans. In *Diving in Animals and Man* (eds A. C. Brubakk, J. W. Kanwisher and G. Sundnes), pp. 33-62. The Royal Norwegian Society of Sciences and Letters, Trondheim.
- Riekkola, L., Andrews-Goff, V., Friedlaender, A., Zerbini, A. N. and Constantine, R. (2020). Longer migration not necessarily the costliest strategy for migrating humpback whales. Aquat. Conserv. Mar. Freshw. Ecosyst. 30, 937-948. doi:10. 1002/agc.3295
- Rogan, E., Cañadas, A., Macleod, K., Santos, M. B., Mikkelsen, B., Uriarte, A., Van Canneyt, O., Vázquez, J. A. and Hammond, P. S. (2017). Distribution, abundance and habitat use of deep diving cetaceans in the North-East Atlantic. Deep Sea Research Part II: Topical Studies in Oceanography 141, 8-19. doi:10.1016/j.dsr2.2017.03.015
- Rojano-Doñate, L., McDonald, B. I., Wisniewska, D. M., Johnson, M., Teilmann, J., Wahlberg, M., Højer-Kristensen, J. and Madsen, P. T. (2018). High field metabolic rates of wild harbour porpoises. *J. Exp. Biol.* 221, jeb185827. doi:10.1242/jeb.185827
- Rojano-Doñate, L., Teilmann, J., Wisniewska, D. M., Jensen, F. H., Siebert, U., McDonald, B. I., Elmegaard, S. L., Sveegaard, S., Dietz, R., Johnson, M. et al. (2024). Low hunting costs in an expensive marine mammal predator. *Sci. Adv.* 10, eadj7132. doi:10.1126/sciadv.adj7132
- Roos, M. M. H., Wu, G.-M. and Miller, P. J. O. (2016). The significance of respiration timing in the energetics estimates of free-ranging killer whales (*Orcinus orca*). *J. Exp. Biol.* 219, 2066-2077. doi:10.1242/jeb.137513
- Santos, M. B., Pierce, G. J., Herman, J., López, A., Guerra, A., Mente, E. and Clarke, M. R. (2001). Feeding ecology of Cuvier's beaked whale

- (Ziphius cavirostris): a review with new information on the diet of this species. J. Mar. Biol. Assoc. U. K. 81, 687-694. doi:10.1017/S0025315401004386
- Sato, K., Aoki, K., Watanabe, Y. Y. and Miller, P. J. O. (2013). Neutral buoyancy is optimal to minimize the cost of transport in horizontally swimming seals. *Sci. Rep.* 3, 2205. doi:10.1038/srep02205
- Schorr, G. S., Falcone, E. A., Moretti, D. J. and Andrews, R. D. (2014). First long-term behavioral records from Cuvier's Beaked whales (*Ziphius cavirostris*) reveal record-breaking dives. *PLoS ONE* 9, e92633. doi:10.1371/journal.pone.0092633
- Schorr, G. S., Hanson, M. B., Falcone, E. A., Emmons, C. K., Jarvis, S. M., Andrews, R. D. and Keen, E. M. (2022). Movements and diving behavior of the Eastern North Pacific offshore killer whale (*Orcinus orca*). Front. Mar. Sci. 9. doi:10.3389/fmars.2022.854893
- Sebens, K. P. (1982). The limits to indeterminate growth: an optimal size model applied to passive suspension feeders. *Ecology* **63**, 209-222. doi:10.2307/1937045
- Shearer, J. M. (2022). The influence of environment on the foraging strategies and physiological ecology of Cuvier's beaked whales (Ziphius cavirostris). PhD dissertation, Duke University, Durham, NC, USA..
- Shearer, J. M., Jensen, F. H., Quick, N. J., Friedlaender, A., Southall, B., Nowacek, D. P., Bowers, M., Foley, H. J., Swaim, Z. T., Waples, D. M. et al. (2022). Short-finned pilot whales exhibit behavioral plasticity in foraging strategies mediated by their environment. *Mar. Ecol. Prog. Ser.* 695, 1-14. doi:10.3354/meps14132
- Silva, M. P., Oliveira, C., Prieto, R., Silva, M. A., New, L. and Pérez-Jorge, S. (2024). Bioenergetic modelling of a marine top predator's responses to changes in prey structure. *Ecol. Evol.* 14, e11135. doi:10.1002/ece3.11135
- Simon, M., Johnson, M. and Madsen, P. T. (2012). Keeping momentum with a mouthful of water: behavior and kinematics of humpback whale lunge feeding. J. Exp. Biol. 215, 3786-3798. doi:10.1242/jeb.071092
- Sinclair, E. H. (2006). Stomach contents of four short-finned pilot whales (Globicephala macrorhynchus) from the Southern California Bight. Mar. Mamm. Sci. 8, 76-81. doi:10.1111/j.1748-7692.1992.tb00127.x
- Skrovan, R. C., Williams, T. M., Berry, P. S., Moore, P. W. and Davis, R. W. (1999). The diving physiology of bottlenose dolphins (*Tursiops truncatus*): II. Biomechanics and changes in buoyancy at depth. *J. Exp. Biol.* **202**, 2749-2761. doi:10.1242/jeb.202.20.2749
- Smith, R. R., Rumsey, G. L. and Scott, M. L. (1978). Heat increment associated with dietary protein, fat, carbohydrate and complete diets in salmonids comparative energetic efficiency. *J. Nutr.* 108, 1025-1032. doi:10.1093/jn/108. 6.1025
- Southall, B. L., Benoit-Bird, K. J., Moline, M. A. and Moretti, D. (2019). Quantifying deep-sea predator–prey dynamics: Implications of biological heterogeneity for beaked whale conservation. *J. Appl. Ecol.* **56**, 1040-1049. doi:10.1111/1365-2664.13334
- Sumich, J. L. (1983). Swimming velocities, breathing patterns, and estimated costs of locomotion in migrating gray whales, *Eschrichtius robustus*. *Can. J. Zool.* **61**, 647-652. doi:10.1139/z83-086
- Svedäng, H. and Wickström, H. (1997). Low fat contents in female silver eels: indications of insufficient energetic stores for migration and gonadal development. *J. Fish Biol.* **50**, 475-486. doi:10.1111/j.1095-8649.1997.tb01943.x
- Torres, W. and Bierlich, K. (2020). MorphoMetriX: a photogrammetric measurement GUI for morphometric analysis of megafauna. JOSS 5, 1825. doi:10.21105/joss.01825
- van Aswegen, M., Szabo, A., Currie, J. J., Stack, S. H., Evans, L., Straley, J., Neilson, J., Gabriele, C., Cates, K., Steel, D. et al. (2025a). Maternal investment, body condition and calf growth in humpback whales. *J. Physiol.* **603**, 551-578. doi:10.1113/JP287379
- van Aswegen, M., Szabo, A., Currie, J. J., Stack, S. H., Straley, J., Neilson, J., Gabriele, C., Cates, K., Baker, C., Steel, D. et al. (2025b). Age-specific body length, mass, and energetic cost of growth in humpback whales. *Marine Ecology Progress Series* 770, 171-194.
- Velten, B. P., Dillaman, R. M., Kinsey, S. T., McLellan, W. A. and Pabst, D. A. (2013). Novel locomotor muscle design in extreme deep-diving whales. *J. Exp. Biol.* **216**, 1862-1871. doi:10.1242/jeb.081323
- Videsen, S. K. A., Simon, M., Christiansen, F., Friedlaender, A., Goldbogen, J., Malte, H., Segre, P., Wang, T., Johnson, M. and Madsen, P. T. (2023). Cheap gulp foraging of a giga-predator enables efficient exploitation of sparse prey. Sci. Adv. 9, eade3889. doi:10.1126/sciadv.ade3889

- Villegas-Amtmann, S., Schwarz, L. K., Gailey, G., Sychenko, O. and Costa, D. P. (2017). East or west: the energetic cost of being a gray whale and the consequence of losing energy to disturbance. *Endang. Species. Res.* 34, 167-183. doi:10.3354/esr00843
- Virtanen, P., Gommers, R., Oliphant, T. E., Haberland, M., Reddy, T., Cournapeau, D., Burovski, E., Peterson, P., Weckesser, W., Bright, J. et al. (2020). SciPy 1.0: fundamental algorithms for scientific computing in Python. *Nat. Methods* 17, 261-272. doi:10.1038/s41592-019-0686-2
- Visser, F., Keller, O. A., Oudejans, M. G., Nowacek, D. P., Kok, A. C. M., Huisman, J. and Sterck, E. H. M. (2021). Risso's dolphins perform spin dives to target deep-dwelling prev. R. Soc. Open Sci. 8, 202320. doi:10.1098/rsos.202320
- Wade, P. R. and Gerrodette, T. (1993). Estimates of cetacean abundance and distribution in the Eastern Tropical Pacific. Rep. Int. Whaling Comm. 43, 477-493.
- Wahrenbrock, E. A., Maruschak, G. F., Elsner, R. and Kenney, D. W. (1974).

 Respiration and metabolism in two baleen whale calves. *Mar. Fish. Rev.* **36**, 3-9.
- Watanabe, H., Kubodera, T., Moku, M. and Kawaguchi, K. (2006). Diel vertical migration of squid in the warm core ring and cold water masses in the transition region of the western North Pacific. *Mar. Ecol. Prog. Ser.* 315, 187-197. doi:10. 3354/meps315187
- Watanabe, Y. Y., Payne, N. L., Semmens, J. M., Fox, A. and Huveneers, C. (2019). Swimming strategies and energetics of endothermic white sharks during foraging. *J. Exp. Biol.* **222**, jeb185603. doi:10.1242/jeb.185603
- Watwood, S. L., Miller, P. J. O., Johnson, M., Madsen, P. T. and Tyack, P. L. (2006). Deep-diving foraging behaviour of sperm whales (*Physeter macrocephalus*). *J. Anim. Ecol.* **75**, 814-825. doi:10.1111/j.1365-2656.2006.01101.x
- Webb, P. W. (1975). Hydrodynamics and energetics of fish propulsion. Bull. Fis. Res. Board of Canada 190, 1-159.
- West, K. L., Walker, W. A., Baird, R. W., Mead, J. G. and Collins, P. W. (2017). Diet of Cuvier's beaked whales *Ziphius cavirostris* from the North Pacific and a comparison with their diet world-wide. *Mar. Ecol. Prog. Ser.* 574, 227-242. doi:10. 3354/meps12214
- West, K. L., Walker, W. A., Baird, R. W., Webster, D. L. and Schorr, G. S. (2018).
 Stomach contents and diel diving behavior of melon–headed whales
 (Peponocephala electra) in Hawaiian waters. Mar. Mammal Sci. 34, 1082-1096.
 doi:10.1111/mms.12507
- Whitehead, H. (2018). Sperm Whale: Physeter macrocephalus. In Encyclopedia of Marine Mammals, 3rd edn. (ed. B. Würsig, J. G. M. Thewissen and K. M. Kovacs), pp. 919-925. Academic Press.
- Wiley, D., Ware, C., Bocconcelli, A., Cholewiak, D., Friedlaender, A., Thompson, M. and Weinrich, M. (2011). Underwater components of humpback whale bubble-net feeding behaviour. *Behavior* 148, 575-602. doi:10. 1163/000579511X570893
- Williams, T. M. (1999). The evolution of cost efficient swimming in marine mammals: limits to energetic optimization. *Philos. Trans. R. Soc. Lond. Ser. B Biol. Sci.* 354, 193-201. doi:10.1098/rstb.1999.0371
- Williams, T. M. and Davis, R. W. (2024). Energetic costs of rest and locomotion in dolphins. In *The Physiology of Dolphins* (ed. A. Fahlman and S. K. Hooker), pp. 9-28. Academic Press.
- Williams, R. and Noren, D. P. (2009). Swimming speed, respiration rate, and estimated cost of transport in adult killer whales. *Mar. Mammal Sci.* 25, 327-350. doi:10.1111/j.1748-7692.2008.00255.x
- Williams, T. M., Davis, R. W., Fuiman, L. A., Francis, J., Le, B. J., Boeuf, M., Horning, M., Calambokidis, J. and Croll, D. A. (2000). Sink or swim: strategies for cost-efficient diving by marine mammals. *Science* 288, 133-136. doi:10.1126/ psinger 298.545.2123
- Wisniewska, D. M., Johnson, M., Teilmann, J., Rojano-Doñate, L., Shearer, J., Sveegaard, S., Miller, L. A., Siebert, U. and Madsen, P. T. (2016). Ultra-high foraging rates of harbor porpoises make them vulnerable to anthropogenic disturbance. *Curr. Biol.* 26, 1441-1446. doi:10.1016/j.cub.2016.03.069
- Wolff, G. A. (1982). A beak key for eight eastern tropical Pacific caphalopod species with relationships between their beak dimensions and size. Fish. Bull. 80, 357-370.
- Wright, B. M., Deecke, V. B., Ellis, G. M., Trites, A. W. and Ford, J. K. B. (2021).
 Behavioral context of echolocation and prey-handling sounds produced by killer whales (Orcinus orca) during pursuit and capture of Pacific salmon (Oncorhynchus spp.). Mar. Mamm. Sci. 37, 1428-1453. doi:10.1111/mms.12836
- Young, R. E. (1978). Vertical distribution and photosensitive vesicles of cephalopods from Hawaiian waters. Fish. Bull. 76, 583-615.

Supplementary Materials and Methods

Thrust Power Validation - Active Vs. Passive Drag

In order to validate the accuracy of our C_T and P_T estimates, we calculated the coefficient of drag $C_{D.active}$ for a swimming cetacean using the following equation from Gough et al. (2021):

$$C_{\text{D.active}} = \frac{P_{\text{T}} - (k_{\text{added}} + 1)M_{\text{body}}(\Delta U/T_{\text{beat}})U_{\text{avg}}}{1/2(\rho S_{\text{a}}U_{\text{avg}}^{3})} \quad (S1)$$

where $k_{\rm added}$ is the coefficient of added mass set at 0.05 for a prolate spheroid of fineness ratio 6.0 (Miller et al., 2004a; Potvin et al., 2021; Skrovan et al., 1999) and $S_{\rm a}$ (m²) is the surface area of each animal estimated from TL using an allometric equation ($S_{\rm a}$ = 0.018TL – 2.14) based on seven species of Delphinidae (Aoki et al., 2017; Bose et al., 990; Curren, 1992). Using these $C_{\rm D.active}$ values, we estimated the mean drag force $P_{\rm active}$; N) for a tailbeat period to be:

$$D_{\text{active}} = \frac{1}{2} \rho S_{\text{a}} C_{\text{D.active}} U_{\text{avg}}^2 + k_{\text{added}} M_{\text{body}} \frac{\Delta U}{T_{\text{beat}}}$$
 (S2)

As a comparison, we used the following equation (Gough et al., 2021; Webb, 1975) to estimate the drag coefficient for a rigid body of a given size as the combination of frictional and pressure drag:

$$C_{\text{D.passive}} = \left[\frac{0.072}{(Re)^{1/5}} \right] * \left[1 + 1.5 \left(\frac{W_{\text{max}}}{TL} \right)^{3/2} + 7 \left(\frac{W_{\text{max}}}{TL} \right)^{3} \right] \quad (S3)$$

here Re is the Reynolds number, a dimensionless value defined as the ratio of inertial to viscous forces:

$$Re = \frac{U_{avg}TL}{T} \quad (S4)$$

The viscosity of water (v; m²s⁻¹) is set at 1.044*10⁻⁶ (Fish, 1998). Using our value of $C_{\rm D.passive}$, we used the standard drag equation (Gough et al., 2021; Webb, 1975) to estimate the mean passive (i.e., parasitic) drag force:

$$D_{\text{passive}} = \frac{1}{2} \rho S_{\text{a}} C_{\text{D.passive}} U_{\text{avg}}^{2} \quad (S5)$$

Finally, we calculated the ratio ($D_{\rm ratio}$) between active and passive drag:

$$D_{\rm ratio} = \frac{D_{\rm active}}{D_{\rm passive}} \quad (S6)$$

Variables and resulting measurements related to our hydrodynamic analyses are provided in Table S3.

Breathing Frequency Methods

Our breathing frequency method relied on the equation:

$$FMR = \frac{1000 * (V_t V_c L C_{\text{total}} R_{\text{resp}} F_{\text{O2}} E_{\text{O2}} C_{\text{O2}})}{60} \quad (S7)$$

which has been used in recent studies to estimate metabolic rates in large whales, including humpback whales (*Megaptera novaeangliae*) and southern right whales *Eubalaena australis*) (Christiansen et al., 2023; Videsen et al., 2023). In this equation, tidal olume (V_t ; L breath⁻¹) ranged from 0.4-0.8 (Fahlman et al., 2016; Wahrenbrock et al., 4), vital capacity (V_c) ranged from 0.8-0.9 (Fahlman et al., 2017; Kooyman, 1973), and oxygen extraction efficiency (E_{O2}) ranged from 0.30 to 0.40 (Videsen et al., 2023). Total lung

capacity ($LC_{\rm total}$; L) was calculated using the allometric equation 0.135*($M_{\rm body}^{.92}$) (Fahlman et al., 2011; Kooyman, 1973), then multiplied by a scaling factor (0.8-1.2) to account for certainty surrounding lung function (Isojunno et al., 2018). Respiration rate (R_{resp} ; eaths·min⁻¹) was allowed to vary by ±10% of the observed average respiration rate for ch deployment to reflect individual and contextual variability in breathing patterns. The ction of oxygen in atmospheric air (F_{O2}) was set at 0.2095 and the calorific coefficient of oxygen (C_{O2} ; kJ L⁻¹) was set at 20.1 (Videsen et al., 2023).

To account for the combined effects of parameter uncertainty on field metabolic rate estimates, we conducted a full sensitivity analysis using all combinations of parameter values within their specified ranges (Figure S3). We then ran a Monte Carlo simulation consisting of 100 iterations (as described in Methods section), where parameter values were randomly sampled from uniform distributions bounded by the same ranges. For each iteration, we computed the total energetic cost over the deployment period and the mean per-second energetic cost of the deployment. This approach allowed us to quantify how uncertainty in respiration-related physiology propagated through to our estimates of energetic expenditure.

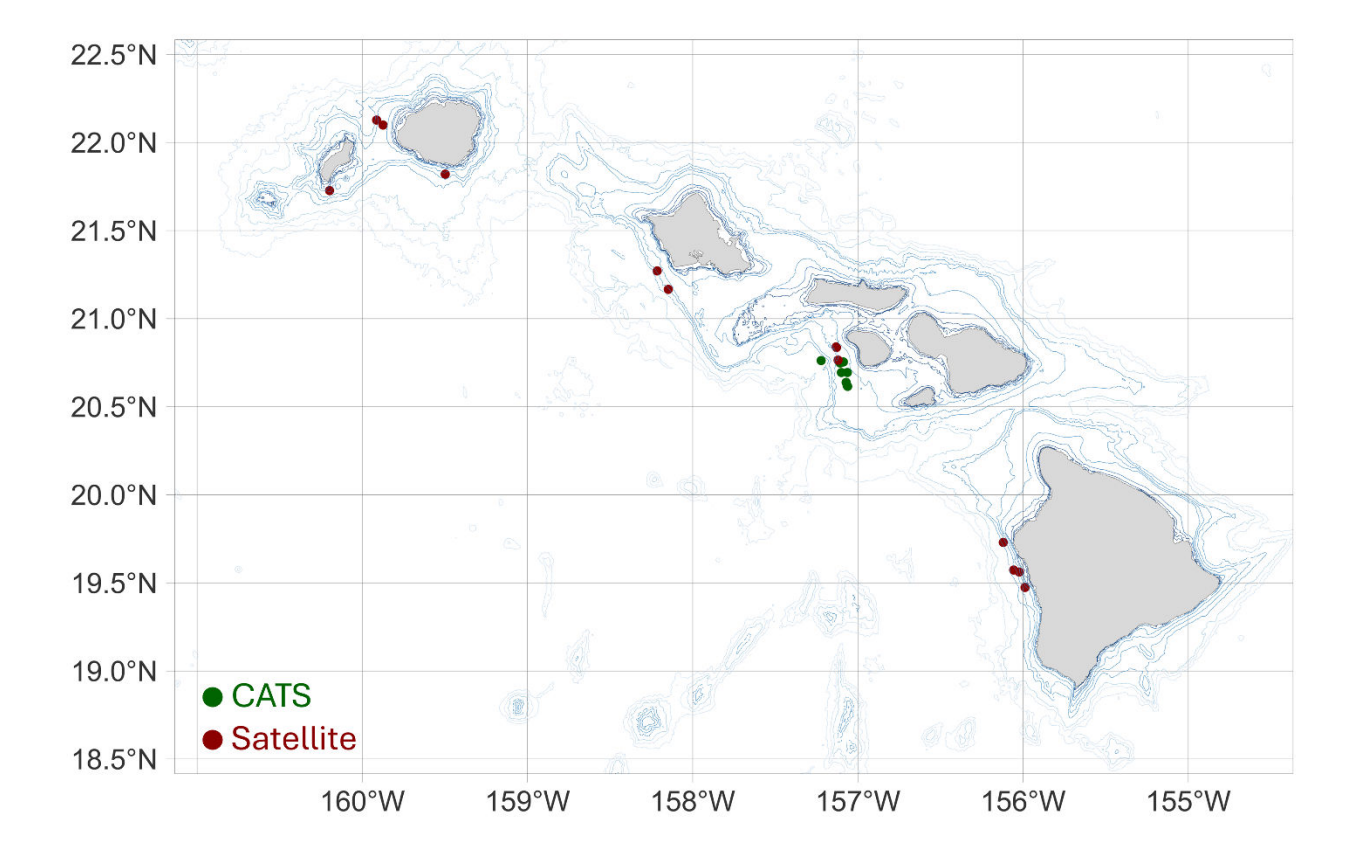


Fig. S1. Map of the main Hawaiian Islands showing the starting locations of our CATS and satellite tag deployments.

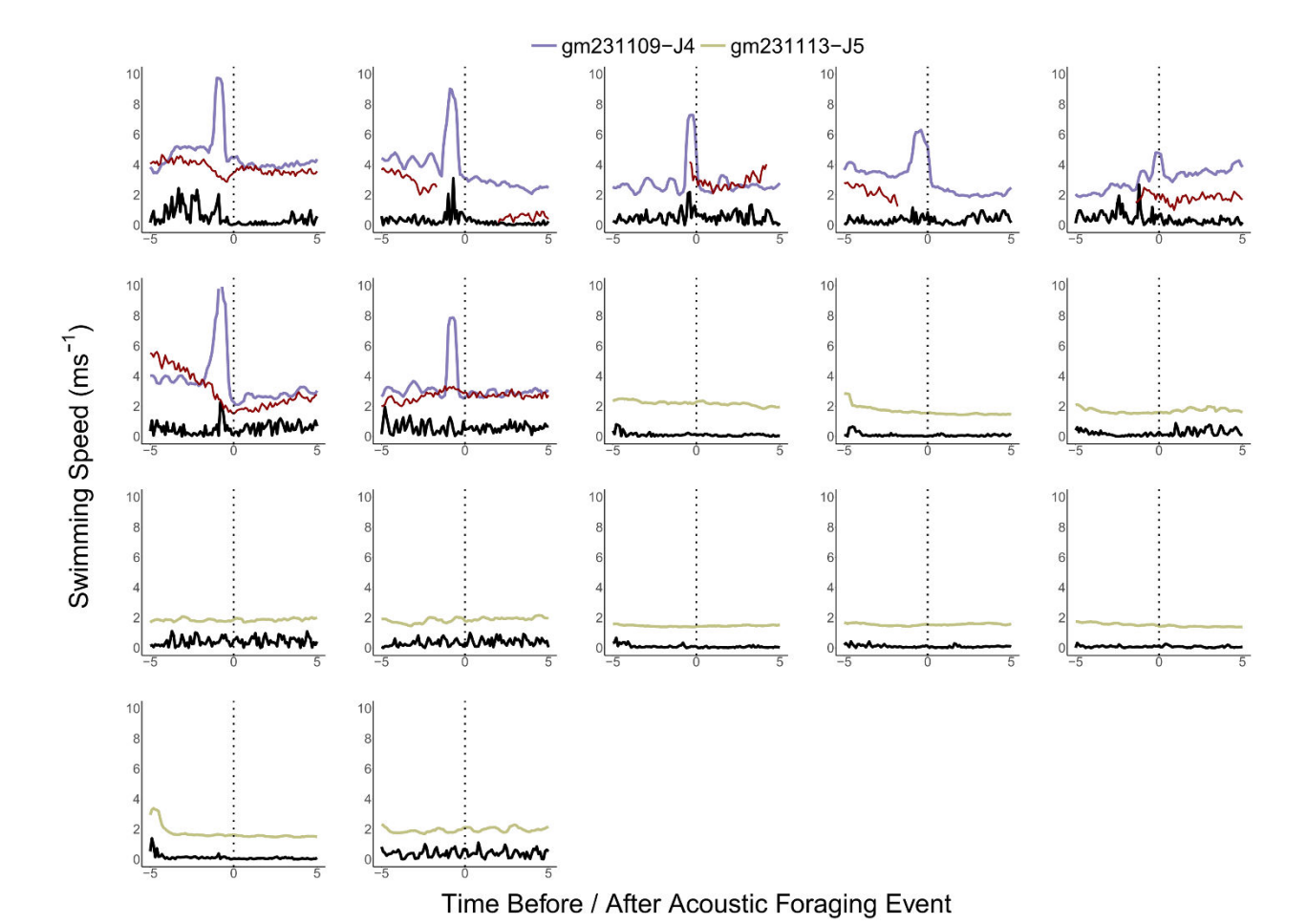


Fig. S2. Period surrounding each foraging buzz in our acoustic dataset (n = 17). The colored lines (blue, green) correspond with the swimming speed, while the black lines correspond with the jerk. The red lines for Gm231109-J4 correspond with a secondary calculation of swimming speed using orientation-corrected depth-rate (OCDR).

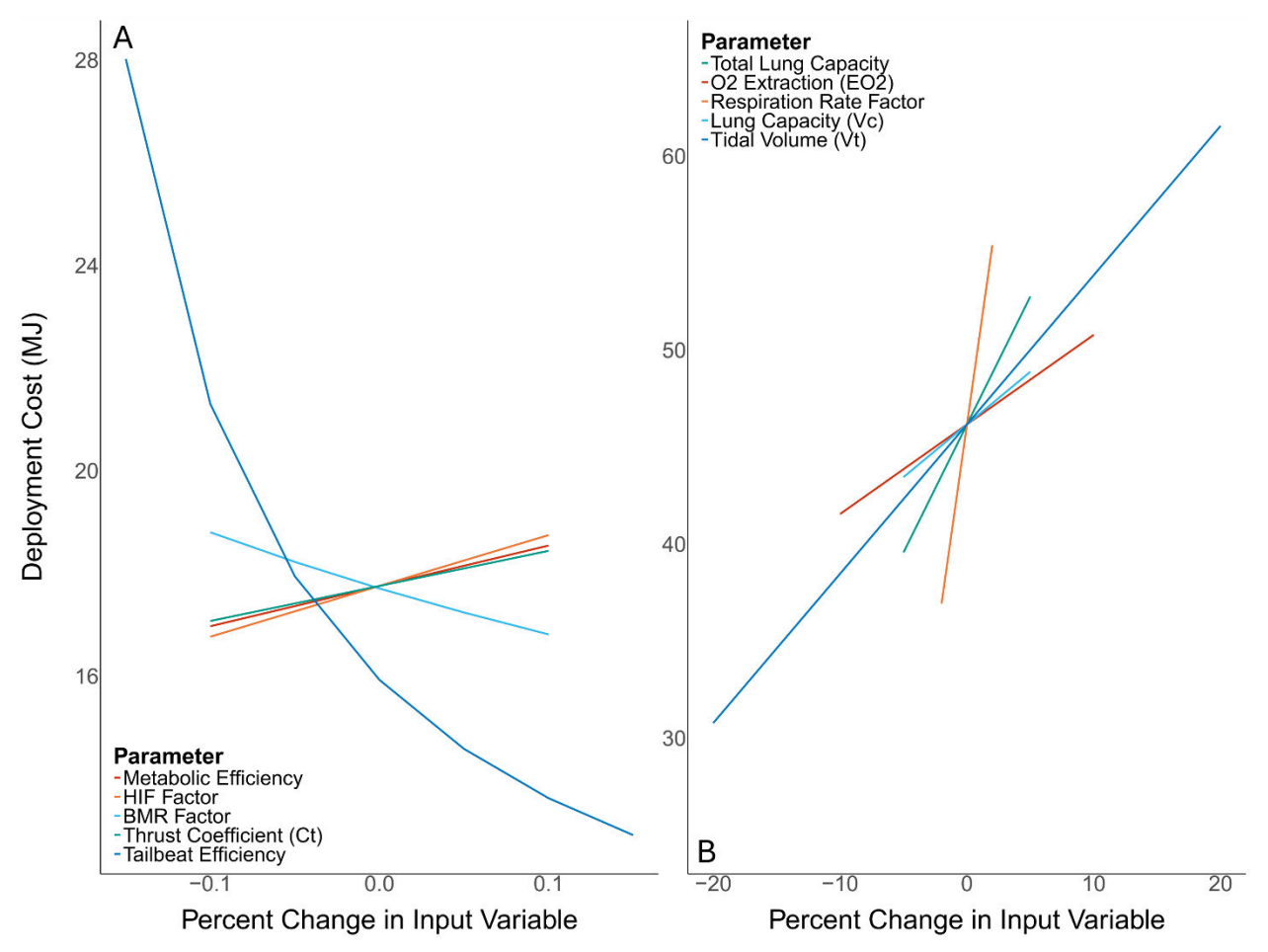


Fig. S3. Sensitivity analyses for model parameters using our thrust (left) and breathing frequency (right) methods.

Table S1. Deployment information for animals tagged with satellite tags.

ID Number	Date	Tag Type	Island	Age Class	Sex	# Days of Behavior Data	Dive Rate (Dives >99.5 m)
GmTag111	12/2/2014	SPLASH 10	Hawai'i	Sub- adult	Male	10.18	48.94
GmTag112	12/4/2014	SPLASH 10	Hawai'i	Sub- adult	Male	19.29	27.06
GmTag118	2/18/2015	SPLASH 10	O'ahu	Adult	Male	18.69	38.52
GmTag121	2/18/2015	SPLASH 10	O'ahu	Adult	Male	17.72	16.54
GmTag133	9/10/2015	SPLASH 10	Ni'ihau	Adult	Male	14.21	39.07
GmTag154	2/14/2016	SPLASH 10	Kaua'i	Adult	Male	8.12	40.38
GmTag169	3/6/2017	SPLASH 10-F	Lana'i	Adult	Male	16.30	38.23
GmTag170	3/13/2017	SPLASH 10-F	Lana'i	Adult	Male	6.69	30.81

GmTag171	3/13/ 2017	SPLASH 10-F	Lana'i	Adult	Male	23.95	23.3
GmTag187	4/17/ 2018	SPLASH 10-F	Hawai'i	Adult	Male	7.68	37.26
GmTag193	4/18/ 2018	SPLASH 10-F	Hawai'i	Sub- adult	Unknown	11.71	42.01
GmTag231	2/9/ 2020	SPLASH 10-F	Kaua'i	Adult	Male	8.50	39.19
GmTag251	2/11/ 2024	SPLASH 10-F	Kaua'i	Adult	Male	13.18	43.93

Table S2. Acoustic metrics (e.g., buzz rate, ICI) taken from selected literature sources related to our analyses.

Species	Reference	Study Site	Avg # of Terminal Buzzes Per Dive / Hour	Non-Buzz ICI	Selected Diving Information
Short-Finned Pilot Whale (Globicephala macrorhynchus)	Current Study	Hawai'i, USA	3.4 ± 0.55 per dive (day)	0.25 ± 0.14 s (descent) 0.2 ± 0.23 s (ascent)	Clicks start at 300 – 400 m (descent) Buzzes in 71% of foraging dives Buzz-adjacent sprints >9 m Sprints >3 in 29% of foraging dives (day)
Short-Finned Pilot Whale (Globicephala macrorhynchus)	Shearer et al. 2022	Cape Hatteras, USA	11.7 – 14.7 per dive (day) 5.3 – 9.7 per dive (night)	-	Sprints >3 m in 55% of foraging dives
Short-Finned Pilot Whale (Globicephala macrorhynchus)	Pederson et al., 2021	Canary Islands, Spain	•	0.34 s (daytime foraging)	-
Short-Finned Pilot Whale (Globicephala macrorhynchus)	Quick et al., 2017	Cape Hatteras, USA	13.2 per dive (State 1 – deep dives) 0 per dive (State 2 – shallow dives)	-	-
Short-Finned Pilot Whale (Globicephala macrorhynchus)	Soto et al., 2008	Canary Islands, Spain	0.6 – 1.5 per dive (day) 4.8 – 5 per dive (night)	-	Clicks start at 300 – 400 m (descent) Buzzes in 72% of foraging dives Buzz-adjacent sprints >9 m Sprints >3 m in 53% of foraging dives (day) Sprints >3 m in 26% of foraging dives (night)
Sperm Whale (Physeter macrocephalus)	Ligurian Sea, Italy + Gulf of Watwood et Mexico, al. 2006 Mexico + Atlantic Ocean, USA		-	Clicks start at 100 – 200 m (descent)	
Sperm Whale (Physeter macrocephalus)	Whale Whale eter 2004 Ligurian Sea, Italy + (descent) 27.7 ± 12.7 per hour (bottom)		(descent) 27.7 ± 12.7 per hour	-	-
Sperm Whale (Physeter macrocephalus)	Zimmer et al. 2003	Ligurian Sea, Italy	-	0.5 – 2.0 s	-
Blainville's Beaked Whale (Mesoplodon densirostris)	Johnson et al. 2006	Canary Islands, Spain	26 – 38 per dive	0.37 ± 0.1 s (searching)	-

Blainville's Beaked Whale (Mesoplodon densirostris)	Johnson et al. 2005	Canary Islands, Spain	Islands, 23 per dive 0.2		Clicks start at 200 – 500 m (descent)
Cuvier's Beaked Whale (Ziphius cavirostris)	Zimmer et al. 2005	Ligurian Sea, Italy	-	0.4 s	
Harbor Porpoise (Phocoena phocoena)	Wisniewska, et al 2018	Denmark	0 – 200 encounters per hour (day) 50 – 550 encounters per hour (night)		Near-continuous feeding
Risso's Dolphin (Grampus griseus)	Arranz et al., 2016	Channel Islands, USA	0 – 52.2 per hour	0.01 s	Relatively shallow foraging depths compared to other deep-diving odontocetes

Table S3. Variables and measurements related to our hydrodynamic calculations of thrust power and drag force. Values are given as mean \pm SD, where applicable.

ID Feathering Number Parameter		Reduced Frequency	Coefficient of Thrust	Propulsive Efficiency	Thrust Power	Reynolds Number	Coefficient of Drag		Drag Force (N)		Active/Passive Drag Ratio	
Number	Parameter	rrequericy	or must	Efficiency	(J s ⁻¹)	Number	Active	Passive	Active	Passive	Drag Kallo	
gm211004- 86	0.67 ± 0.0007	0.54	0.214 ± 0.0002	0.85 ± 0.0003	154.86 ± 0.49	5584874	0.018 ± 0.0001	0.004	85.28 ± 0.25	23.04	4.89 ± 0.01	
gm211006- 87	0.58 ± 0.0022	0.79	0.526 ± 0.0012	0.87 ± 0.0008	36.20 ± 0.35	2573890	0.033 ± 0.0003	0.004	30.01 ± 0.25	7.27	7.19 ± 0.06	
gm221116- J2	0.53 ± 0.0003	0.69	0.372 ± 0.0001	0.89 ± 0.0001	457.34 ± 0.53	7023802	0.036 ± 0.0000	0.003	274.00 ± 0.31	27.88	10.63 ± 0.01	
gm231109- J4	0.74 ± 0.0012	0.61	0.270 ± 0.0004	0.85 ± 0.0004	52.39 ± 0.18	3550350	0.020 ± 0.0001	0.004	33.78 ± 0.11	13.11	4.62 ± 0.02	
gm231110- J6	0.83 ± 0.0013	0.48	0.144 ± 0.0003	0.83 ± 0.0004	168.97 ± 0.65	6845646	0.010 ± 0.0000	0.004	69.89 ± 0.30	35.12	2.85 ± 0.01	
gm231113- J5	0.85 ± 0.0012	0.51	0.139 ± 0.0003	0.81 ± 0.0003	193.16 ± 0.66	7079856	0.010 ± 0.0000	0.004	83.34 ± 0.32	34.26	2.73 ± 0.01	
gm240409- J3	0.75 ± 0.0012	0.59	0.220 ± 0.0004	0.82 ± 0.0004	126.40 ± 0.52	5431376	0.014 ± 0.0001	0.004	65.07 ± 0.28	21.94	3.82 ± 0.02	
gm240409- J4	0.53 ± 0.0011	0.81	0.509 ± 0.0007	0.87 ± 0.0005	350.18 ± 1.70	6465011	0.038 ± 0.0002	0.004	220.11 ± 1.03	25.78	10.35 ± 0.05	
Mean ± SD	0.68 ± 0.13	0.63	0.299 ± 0.15	0.85 ± 0.03	192.44 ± 144.13	5569350	0.022 ± 0.012	0.004	107.69 ± 89.55	23.55	5.88 ± 3.17	